TR-60-266

THE UNIVERSITY OF CHICAGO
DEPARTMENT OF METEOROLOGY

TECHNICAL NOTE No. 21
CLOUD PHYSICS LABORATORY

CLOUD REFRACTIVE INDEX STUDIES

PART III

Final Report under Contract No. AF 19(604)-1931

by

Edward L. Harrington

Chicago, Illinois
May 2, 1960

The research reported in this document was sponsored by the Geophysics Research Directorate of the Air Force Cambridge Research Center, Air Research and Development Command, under Contract No. AF 19(604)-1931.

THE UNIVERSITY OF CHICAGO
DEPARTMENT OF METEOROLOGY

TECHNICAL NOTE NO. 21

CLOUD PHYSICS LABORATORY

CLOUD REFRACTIVE INDEX STUDIES

PART III

Final Report Under Contract No. AF19(604)-1931

by

Edward L. Harrington

Chicago, Illinois
May 2, 1960

The research reported in this document was sponsored by the Geophysics Research Directorate of the Air Force Cambridge Research Center, Air Research and Development Command, under Contract No. AF19(604)-1931.

ABSTRACT

Statistical analysis of refractive index gradients has been applied to some measurements made in the sub-cloud layers at altitudes from 1,000 ft to 3,000 ft over the Caribbean Sea. The data were arranged in bivariate frequency tables of $\triangle N$ versus $\triangle S$ and tests were made to determine if these distributions changed with respect to altitude and horizontal location, and to see if the distributions representing cloud air were different from the clear-air distributions. The tests revealed a high degree of sampling variability which masked any other variability which might be present. The distributions of $\triangle N$ show that over ninety per cent of the values are less than one N unit, reflecting the high humidity encountered at these altitudes.

Autocorrelograms of three low-altitude passes are inconclusive because lag sizes were too large to detect the gradient activity and the records were too short for meso-scale variation to be verified. The correlogram for a record of data gathered entirely in clear air showed high positive correlation over a distance of approximately 28 km.

The integrated refractive index change along the aircraft flight path in cloud has been computed for a number of clouds from both the subtropical oceans and the continental United States. The mean behavior of this integral function is shown for the tropical ocean clouds. A difference in the size distribution of the integral function between

the ocean and continental clouds is examined and attributed to a biased sampling of the ocean clouds with respect to cloud-environment refractive index difference.

Gross refractive index measurements have been made on additional cloud samples.

TABLE OF CONTENTS

LIST OF ILLUSTRATIONS

LIST OF ILLUSTRATIONS (CONTINUED)

LIST OF ILLUSTRATIONS (CONTINUED)

LIST OF ILLUSTRATIONS (CONTINUED)

SECTION I

INTRODUCTION

For the past several years the Cloud Physics Laboratory has been analysing measurements of refractive index made with an airborne refractometer in and in the vicinity of convective clouds. The refractive index measurements were made by Dr. R. M. Cunningham of the Geophysics Research Directorate, Air Force Cambridge Research Center during the years 1955-1956 in clouds over the continental United States, the Baham Islands, and the Caribbean Sea south of Puerto Rico For the most part, analysis work at the University of Chicago has been concerned with the clouds situated in the Bahama-Caribbean Region Some of the final analysis has included continental clouds, primarily for comparison purposes.

The present report is the first of two final reports summarizing the refractive index investigations. Two previous reports (1) and (2) described data reduction techniques and presented two types of analysis, one micro-scale and one on a scale of the order of cloud dimensions. The material presented here represents a continuation of this two-fold approach, although the analysis techniques are different and some different parts of the atmosphere are considered.

One type of analysis originated by Cunningham and continued by the University of Chicago is the measurement of gross, or cloud-scale refractive index features. These include such measurements as the refractive index difference between cloud core and environment, cloud sizes, transition zone sizes, and related features. These measurements have been made for additional clouds and are presented in this report.

A considerable amount of attention has been given to the refractive index behavior at altitudes lower than those considered in previous work, in particular, the layer of the atmosphere between the altitude of cloud bases and a level approximately 1,000 ft above the ground (sea surface). The refractive index records obtained at these altitudes were studied by means of the gradient technique of (1) and (2) and by autocorrelation analysis.

A specific problem, that of the cumulative effect of refractive index turbulence on a line passing through a cloud, was examined using statistical methods.

Statistical techniques have been employed throughout the refractive index analysis. In particular, tests of significance such as the t-test, rank tests, and tests using chi-square have been employed and frequent reference is made to them in the text. These tests and their use are described in textbooks in Statistics of which (4) is just one of the many to which the reader might refer.

Most of the analysis presented in this report was undertaken to meet various requirements of the Air Force. In the course of the analysis some problems have appeared which hold particular interest for meteorologists. It is proposed to consider some of these in the second of the two final reports.

SECTION II

LOW ALTITUDE ANALYSIS

A. Refractive index gradient behavior at low altitudes

On several of the late 1956 flights in the Caribbean Area refractive index measurements were made at altitudes corresponding to the height of cloud bases and lower. To make these measurements the aircraft was flown for periods of time of the order of minutes on constant headings with the Sanborn Recorder running at a fast speed. At the highest of these low altitude passes (2,000 to 3,000 ft) some clouds were penetrated very near to their bases. On the lower passes (1,000 ft) no cloud was intercepted, but the aircraft often flew through precipitation areas.

Seven of the low altitude passes from the flights of 28 November and 30 November were chosen to be analyzed. Table 1 summarizes the passes. The 28 November flight was assigned the identification number 4 and that of 30 November the number 5.

Fig. 1 and 2 show the relative flight paths of the aircraft during the low altitude passes with cloud penetrations identified. The flight paths are presented to emphasize the lateral proximity of the passes on each day.

Photographs of clouds associated with two of the passes are presented in fig. 3 and 4.

TABLE 1. SUMMARY OF LOW ALTITUDE PASSES

Date	Pass No.	Altitude (feet)	Path Length (km)	RI Range N units	Controller-Observer's Remarks
28 Nov. 1956	4-1	2000	2.3	12.9	A/c skimming cloud bases
	4-2	2000	3.5	9.2	A/c skimming cloud bases, occasional penetration
	4-3	2000	8.3	9.2	Under fracto-cu, entered base of "sizeable cu"
	4-4	2000	4.1	8.4	Rainbow; entered light drizzle just below base
	4-5	2000	16.0	11.6	Entered light drizzle then moderate rain and scud
	4-6	1000	4.7	6.5	No comments
	4-7	1000	16.0	11.6	Entered rain area under cloud with anvil top
30 Nov. 1956	5-1	3000	19.5	15 7	Entered cloud with "lots of breaks," strato-cu
	5-2	2500	11.3	10.6	Entered light drizzle, generally below cloud bases
	5-3	1000	27.6	11.1	Under bases of cu and strato-cu

The refractive index measurements of the low altitude passes were subject to two types of analysis: (1) an examination of the statistics of refractive index gradients similar to the examination made for cloud penetrations made at the higher altitudes (2), and (2) autocorrelation analysis.

The technique of data reduction for the refractive index gradients (or more properly increments of refractive index change $\triangle N$ and the space increments $\triangle S$ over which they are measured) was identical to that described in previous reports. Bivariate frequency distribution tables of $\triangle N$ and $\triangle S$ were compiled and examined with respect to the altitude of measurement and with respect to cloud air and clear air.

The problem of separating clear air from cloud air has been treated somewhat differently from previous analysis. For passes through clouds at higher altitudes the refractive index record had a shape which enabled the analyst to designate regions as clear air, transition, or cloud core in an almost purely objective manner. At lower altitudes the high environment humidities made for a much less obvious indication of cloud boundaries.

Besides the refractometer records, two other kinds of data were present which indicated the type of air which the aircraft instruments were measuring. The observations of the flight-controller scientist, as indicated by his comments on a tape record and by a signal into a line recorder, were one. The other was provided by an Australian liquid-water

content instrument. The controller's signals were of two kinds: an indication of the points of cloud entry and exit, and a similar signal for entry and exit of rain areas. A discussion of the ability of an aircraft passenger to record cloud boundaries appears in the appendix.

When refractive index records were evaluated and the values of refractive index entered on punched cards, each card was coded to indicate if the data point was in-cloud according to any one of the following criteria or of any combinations of them:

1. the pattern of the refractive index record
2. the controller's in-cloud signal
3. the controller's rain signal or voice comments on the presence of rain
4. indication of liquid water by the Australian instrument

Absence of any of these was taken as indication that the aircraft was in cloud-free air and the data point was so coded.

After the computation of ΔN and ΔS the data cards for each pass were sorted into three groups: (1) those points about which there was no doubt that they represented clear air, (2) those points which we were certain were in cloud air and, (3) all other points. Group three consisted of the data points which were coded according to the refractometer trace but which had no other indication of being in-cloud. For each pass the points in this group were re-examined along with the refractive index data record and recorded voice comments, and it was then decided, subjectively, whether

to consider them as cloud air or clear air.

Having grouped the data according to their presence in cloud air or clear, they were further grouped according to the altitude at which the measuring passes were made. Two such groups were made, one for the passes at or near 1,000 ft, and one for those at 2,500 and 3,000 ft. Bivariate distributions of $\triangle N$ versus $\triangle S$ were then compiled for each of these four groups. In these distributions the absolute value of $\triangle N$ is considered. The marginal distributions are presented in fig. 5, 6, 7, and 8. Table 2 presents distributions of $\triangle N$ values for $\triangle S$ measured below the resolution of the data reduction equipment. Examination of the frequency distribution curves suggests no difference in gradient intensity or size distribution between the two altitudes or between the cloud air and the clear air. The distributions of refractive index increments show in all cases that about ninety per cent of the $\triangle N$ values are less than one N unit. This is a manifestation of the high humidities of the lower altitudes which allow less freedom for refractive index variations. This phenomenon is anticipated to a certain extent by the small values of the range of refractive index change for each of the low altitude passes (table 1).

In order to see if the distributions of $\triangle N$ versus $\triangle S$ underwent any significant change with respect to altitude or spatial change, it was decided to examine them with the aid of statistical tests of significance What was done was to treat the frequency distribution class intervals as

columns in a contingency table and the data groups to be examined (samples from individual passes, altitude groups, cloud and clear air) as rows. Chi-square for each box could then be computed and the total chi-square examined at the appropriate level of significance (we chose 5 per cent) Such a test could be performed on either the marginal distributions or the bivariate distributions themselves.

TABLE 2. DISTRIBUTION OF VALUES OF $\triangle N$ MEASURED OVER FLIGHT PATH INTERVALS LESS THAN THE MINIMUM RESOLUTION OF THE DATA REDUCTION SYSTEM

$\triangle N$	Clear Air	Cloud Air
0.0 - 0.4	73	163
0.5 - 0.9	37	78
1.0 - 1.4	4	13
1.5 - 1.9	2	5
2.0 - 2.4		2

The purpose of making tests of significance in distributions of $\triangle N$ versus $\triangle S$ was to answer the question: Are there significant differences in the distributions of refractive index increments with respect to their space sizes when the sample distributions are from populations respectively: (1) at different vertical positions (2) at different horizontal positons and (3) in clear air and in-cloud? With the possible exception of (2) our data lend themselves to seeking answers to this problem. On each day the sampling passes were separated by differences of the order of a few miles (fig. 1 and 2). On a synoptic scale

these horizontal distances might be insignificant while on a meso-scale they might be important. As will be seen below, the tests make this point merely academic.

The hypothesis tested by a contingency table chi-squre computation is that of independence, i.e., that the data distribution by columns (here the class intervals of ΔN and ΔS) is independent of the distribution by rows (the various passes for example).

The first data to be tested were the distributions of passes 4-1 through 4-5. These measurements were made at the same altitude on 28 November 1956. The chi-square test on these data rejected the hypothesis of independence at a highly significant value ($P \quad 0.0005$) both for clear air and cloud air. This would seem to say that each of the samples was unique.

The next step was to test passes 4-2 and 4-5: these passes were separated by approximately 6 km in air space. Here too, the hypothesis was rejected For clear air P lay between 0.001 and 0.005 and for cloud air P was less than 0.0005.

Two more such tests were made. All of the clear-air data for the 2,000 ft passes were pooled and compared with the cloud-air data for the same altitude, and finally the cloud-air and clear-air distributions for 2,000 ft were compared with those of 1,000 ft In both cases the hypothesis of independence was again rejected.

Apparently any systematic variation in the distribution of N versus S within the small regions of the atmosphere which we are

considering here is either absent or indistinguishable from the variability among the samples as treated in our testing framework. A lack of variation in the distributions over altitude changes of 1,500 ft should not be surprising. Where altitude variation has been shown (1, 2), the altitude ranges have been of the order of thousands of feet rather than hundreds. Indeed data taken at altitudes separated by 1,000 ft were often combined and considered to represent a single median altitude

The data for all passes in pooled form are presented in Appendix I. Only the cloud- and clear-air identity has been maintained. Once again the difference between two distributions is highly significant statistically. In this case, however, it may be safe to draw some more nearly enlightening conclusions.

An examination of the two distribution tables reveals that the largest differences between them lie among the "limb" boxes. For ΔS values less than 5 meters the largest ΔN's are more frequently found in the cloud samples. For small values of ΔN the larger ΔS values predominate in the clear air. This seems reasonable. Our rules for separating cloud air from clear air have caused us to label any low-level analogue of the transition zone as cloud air. Previous work has shown that the larger ΔN values measured over small distances (larger gradients) are most frequent in the transition zones. Small values of the refractive index gradient usually are most frequent in the clear air.

B. Autocorrelation of low altitude refractive index records

A different approach to the examination of refractive index behavior at the lower altitudes is that of autocorrelation analysis. Autocorrelation coefficients were computed for low altitude passes 4-7 and 5-3 and a pass from another flight, that of 20 November. The latter pass was made under conditions similar to those of the low altitude passes discussed in the preceding paragraphs.

For all three runs the correlation coefficients were computed for lag units of 0.1 sec of refractive index record. A second set of coefficients were computed for run 4-7 using lag units of 1 sec. The choice of these lag sizes was dictated by convenience of data reduction.

It is generally agreed that in autocorrelation analysis the maximum number of lags should not exceed 25 per cent of the total length of the record under consideration. Some statisticians, with whom the author has been able to discuss the problem, suggest the optimum number of lags is about 5 per cent. As a compromise we chose 10 per cent for these computations.

Since we are using a time-series analysis tool to examine a spatial quantity, the lags are converted to flight-path length using the mean air speeds of the respective runs. At B-29 air speeds a lag of 0.1 sec may be thought of as corresponding to 10 m of flight path. By reading the data record at such an interval we exclude most of the gradient-scale refractive index activity. In the tables of Appendix 1

approximately 90 per cent of the cloud-air gradients are measured over distances of less than 10 m. The 1 sec lag unit precludes the consideration of all the data in Appendix I and all but a trivial number of the gradient sizes encountered in the previous gradient studies.

Fig. 9 and 10 present the correlograms. Table 3 presents a summary of the flight data associated with the passes. We can see from the figures that the correlograms have detected no periodic phenomena. Perhaps the beginnings of a cycle are indicated by the correlogram for 20 November. It is interesting to note that for pass 5-3 which was made entirely in cloud-free air, very high positive correlation is maintained through the region for which the correlation coefficients were computed. It would seem reasonable to expect that any periodicity that appeared would have wave lengths of the order of the distance between clouds. The 20 November pass made 4 penetrations into cloud air. If the negative part of that correlogram is indeed half a wave length of oscillation, the wave length of approximately 3 km which it suggests would certainly be a reasonable figure for cloud spacing.

TABLE 3. SUMMARY OF AUTOCORRELATION PASSES

Pass	Altitude (feet)	Path Length per 0.1 sec	Path Length Total	No. of Clouds Entered	Path Length In Cloud
20 Nov. 1956	2400	9.9 m	27.9 km	4	350 m
4-7	1000	9.0 m	16.0 km	2*	4600 m
5-3	1000	8.6 m	27.6 km	0	0

*A/c passed through a rain shower below cloud bases.

It is evident from the correlograms that the atmospheric variations which govern the refractive index variation as measured here are on a scale which runs from between-cloud distances down to the meso-scale distances. The near identity of the two correlograms for pass 4-7 demonstrates that 0.1 sec lag at B-29 air speeds is a much smaller unit than is necessary to examine this type of refractive index activity. On the other hand, the 0.1 sec lag is too large by perhaps a factor of 4 to furnish an autocorrelogram of the refractive index variability which has been examined in gradient studies.

SECTION III

THE INTEGRATED REFRACTIVE INDEX CHANGE ALONG THE AIRCRAFT FLIGHT PATH WITHIN A CLOUD

A. Introduction

The effect exercised by a field of refractive index gradients upon a ray passing through it is cumulative, being integrated along the path of the ray, starting at the boundary of the field. In this section we propose to examine statistically this integrated refractive index change along a line. The line is that of the aircraft flight path. The refractive index gradient field is that of cloud air, both transition and core.

The function which we consider is $\int \Delta N dS$, where S is distance along the flight path from the inbound cloud edge ΔN is the difference between the refractive index at any point within the cloud and that of the environment at the cloud edge. Fig. 11 shows schematically $\int \Delta N dS$ with respect to the refractometer records as the aircraft penetrates a cloud. The value of the function $\int \Delta N dS$ at a distance S from the cloud edge is the area bounded by the trace of the refractive index record, a horizontal line at zero ΔN, and a vertical line at distance S. The dimensions of the functions are N-unit meters.

B. Computation methods

Computations of ΔNdS have been made for two groups of clouds, a sample from the Bahama flights of summer 1956 and a sample from the continental flights of 1955.

The clouds chosen for the computations of $\int \Delta NdS$ from the 1956 flights were those for which refractive index gradients had been computed by machine methods. For these clouds values of gradient ΔN and ΔS already existed on punch cards. To arrive at $\int \Delta NdS$ the problem was essentially to sum the gradient ΔN's and ΔS's after the cards were placed in proper sequence. This was accomplished on the University of Chicago's Univac.

In evaluating $\int \Delta NdS$ for the 1955 clouds, areas under cloud deflections of the refractive index records were measured by means of the Benson-Lehner "Oscar".

C. Mean behavior of $\int \Delta NdS$

In analyzing the results of the computations of $\int \Delta NdS$, it has been our purpose to attempt to determine what values of the integral might be expected at selected points in the atmosphere with reference to altitude and horizontal distance from the cloud edge.

Fig. 12 through 23 present mean values of the function $\int \Delta NdS$ for the first 200 m of cloud flight path by altitude groups. Also shown in these figures are the extreme values of the function for each sample for which the mean is computed.

The data in fig. 12 through 17 are from the summer flights of 1956. The 4,000 ft clouds are from the 19 June flight, the 9,000 ft clouds from the 21 June flight, and the remainder from the flight of 15 June.

There are clouds in which the integral function is seen to be negative over part or all of the flight path segment (200 m) shown in the figures. This is an indication of values of refractive index within the cloud which are lower than the refractive index at the cloud edge. In many cases this probably indicates an error in determining the exact point at which the aircraft entered the cloud. Although in most cases clouds are exactly defined by the shape of the refractometer record, there are exceptions and in these cases other factors must be considered in order to locate the cloud edge. The exceptions are generally of two kinds. When the aircraft penetrates clouds at low altitudes with high environment humidity and a large amount of refractive index turbulence in the environment air, it is often difficult to pick the exact break in the refractive index record which identifies the cloud boundary. At the highest altitude of cloud penetration, where there is negligible change in refractive index from environment air to cloud air, there is no break in the refractive index record to identify the cloud edge. In these cases the cloud edge is determined from the signal given by the controller-observer, riding in the nose of the aircraft. This signal may be in error by more than $\pm$ 1/2 sec (Appendix II) for several reasons, most important of which are difficulty in making the decision of the precise moment of aircraft entry into cloud and the time lag in putting the signal in the record once the decision has been made. At B-29 air speeds 1/2 sec corresponds to a distance of approximately 50 m.

In order to demonstrate an altitude variation in the integral function, all of the mean curves for the summer 1956 clouds are presented in fig. 24. Although the sample for which the mean functions have been computed are selective, we may generalize on a few aspects of the figure.

Among other things the integral functions reflect the state of environment-saturation refractive index difference. We shall see later that, unfortunately, our sample of clouds is biased with respect to this measurement. However, the variation with altitude of environment-saturation refractive index difference is demonstrated rather well here. One may expect fo find the largest values of environment-saturation refractive index difference where convective clouds have penetrated dry inversions--the trade-wind inversion in the case of these clouds over the Bahamas. The maximum mean value of the integral at 6,000 ft in fig. 24 might be considered to demonstrate this, although the 6,000 ft data were acquired on a day (15 June 1956) when the trade-wind inversion was relatively weak (1). The 4,000 ft data (from the flight of 19 June) were acquired in the relatively high humidity region below a strong trade-wind inversion. The remaining functions decrease in value with altitude in a way which follows decreasing environment-saturation refractive index difference.

To say that the integral function reflects the amount of refractive index change from environment to core (saturation) does not tell the whole

story. The question of how much saturated air is included in the first two hundred meters of cloud flight path still remains. This problem will be dealt with in another part of this discussion. Let us merely state here that, except for extremes in altitude difference, the size of the transition zone is relatively insensitive to altitude variation.

Another way of examining the mean behavior of the integral function may be seen in fig. 25. Here isopleths of $\int \Delta N dS$ are presented on an altitude-distance graph, based on the mean measurements of the clouds over the Bahamas. In fig. 26 are drawn isopleths of the value of the ΔN of the integral function, that is the mean refractive index increase above environment refractive index at the cloud edge. This is, of course, the derivative of the integral function along the aircraft flight path. From this figure we may infer that the integral function will undergo its greatest increases in the lower altitudes, although not necessarily at the lowest. This is merely a restatement of the fact that the largest environment to cloud refractive index differences will be found near the trade-wind inversion. Along a given flight path the largest value of ΔN will of course be found in the cloud core and this is shown, except for the lower altitudes, by an increase in ΔN with distance into the cloud. In the lower altitudes many of the cloud cells examined were less than 200 m in extent. The closed isopleth with the value of 8 N-units demonstrates that there were a sufficient number of these clouds in the ample to show a mean decrease in ΔN with distance beyond approximately 120 m.

For the purpose of examining more closely the behavior of the integral function at the cloud edge, the mean values of ΔN and $\int \Delta NdS$ for the first 40 m of cloud flight path are shown in tables 4 and 5. For each altitude group the first 40 m has been divided into 4 class intervals. Means have been computed of all cloud measurements falling in these class intervals. The means and the sample standard deviations are presented in tables 4 and 5.

D. $\int \Delta NdS$ in ocean clouds and clouds over the continent

The clouds which are represented in fig 18 through 23 were measured on four of Cunningham's flights over the United States in June and July 1955. The clouds for 30 June were found 30-50 miles northwest of Boston. On 17 July clouds were measured between Bedford, Massachusetts and Wright-Patterson Air Force Base, Ohio. The 19 July clouds were found northeast of Tucson and the 31 July clouds were found in the vicinity of the Arizona-California border.

Because of the geographical diversity of the continental clouds, the data for each flight are presented separately. In presenting the data for 19 and 31 July, the integral function has been averaged over a larger altitude layer than it was for the Baham clouds. This was done to obtain suitable sample sizes.

We wish to compare the integral function in the clouds over the United States, which we shall designate as "continental", with that of

TABLE 4. MEAN ΔN IN FIRST 40m OF CLOUD, BY ALTITUDE GROUPS AND 10m CLASS INTERVALS OF FLIGHT PATH. (σ = Standard Deviation)

Altitude Group (feet)	1 - 9m Sample Size	1 - 9m Mean (N units)	1 - 9m σ	10 - 19m Sample Size	10 - 19m Mean (N units)	10 - 19m σ	20 - 29m Sample Size	20 - 29m Mean (N units)	20 - 29m σ	30 - 39m Sample Size	30 - 39m Mean (N units)	30 - 39m σ
4000	28	0.9	0.8	44	2.6	2.0	39	4.2	2.8	40	5.3	3.1
5000-7000	11	0.6	1.3	19	3.0	3.1	13	5.3	4.6	20	6.9	3.7
9000	4	0.7	0.8	6	1.7	1.6	6	3.7	1.4	5	3.5	1.5
13000-19000	9	0.3	1.0	10	1.0	1.3	12	0.5	0.8	11	0.9	0.8
21000-25000	4	0.2	0.2	13	0.2	0.2	11	0.5	0.6	9	0.5	0.8

TABLE 5. MEAN $\int \Delta N dS$ IN FIRST 40m OF CLOUD, BY ALTITUDE GROUPS AND 10m CLASS INTERVALS OF FLIGHT PATH (σ = Standard Deviation)

Altitude Group (feet)	1 - 9m Sample Size	1 - 9m Mean (N units)	1 - 9m σ	10 - 19m Sample Size	10 - 19m Mean (N units)	10 - 19m σ	20 - 29m Sample Size	20 - 29m Mean (N units)	20 - 29m σ	30 - 39m Sample Size	30 - 39m Mean (N units)	30 - 39m σ
4000	28	4.5	4.0	44	26.0	20.0	39	68.4	42.2	40	121.8	78.2
5000-7000	11	3.4	7.2	19	21.3	28.7	13	63.2	17.2	20	139.6	98.1
9000	4	5.1	5.4	6	17.4	18.2	6	54.7	34.7	5	87.6	47.1
13000-19000	9	1.4	3.6	10	10.4	12.6	12	14.0	21.7	11	23.6	24.9
21000-25000	4	1.4	1.3	13	2 5	2.2	11	9.1	9.4	9	11.2	12.2

the clouds from the Bahama flights, which we shall designate as "ocean" clouds. For the purpose of comparison we consider as a statistic the value of $\int \Delta NdS$ at a point 200 m from the cloud edge. Fig. 27 shows the values of $(\int \Delta NdS)$ 200 m from the two cloud populations with respect to the altitude at which they were measured The sample from ocean clouds is seen to be distributed about smaller median values than that of the continental clouds. This is true whether we consider the samples as a whole or separate them into "low" altitude and "high" altitude groups, the boundary between high and low altitudes being placed somewhat arbitrarily at 12,000 ft. Tests performed on these sample distributions show that the difference in medians between continental and ocean clouds is statistically significant.

There are two possible explanations for the apparent tendency toward larger values of $(\int \Delta NdS)$ 200 m in clouds over the continent. If transition zones are less than 200 m in size more often in the continental clouds, then in sampling at 200 m we have sampled transition air more often in the ocean clouds making for smaller values of the integral in these clouds. If cloud-environment refractive index differences are less for over-ocean clouds than for clouds over the continent, then the integral function will be less for the ocean clouds at all distances.

Tables 6 and 7 show distribution of the sizes of transition zones for all of the clouds for which refractive index measurements have been made. These include both inbound and outbound zones. Table 8 presents

TABLE 6. DISTRIBUTION OF TRANSITION ZONE SIZES, OCEAN CLOUDS

Altitude, feet	0 < 100m	100-199m	200-299m	300-399m	400-499m	500-599m	600-699m	700-799m	800-899m	900-999m	>999m	Clouds Entirely Transition		Total
3000	2	9	6	2	1	1					1			22
4000	1	11	5	7			1							25
5000		8	4	2	3	2	1				1			21
6000-7000	21	59	42	17	6	8	1	3			1	2		160
8000-9000	6	25	16	8	4	3		1						63
10000-12000	2	12	10	6	1					1				32
13000-14000	3	5	5	1	1		1		2					18
17000		6	2	3	2	1		2			4			20
18000-19000	1	4	3	2	1						1			12
Total	36	139	93	48	19	15	4	6	2	1	8	2		373

TABLE 7. DISTRIBUTION OF TRANSITION ZONE SIZES, CONTINENTAL CLOUDS

Altitude, feet	0 < 100m	100-199m	200-299m	300-399m	400-499m	500-599m	600-699m	700-799m	800-899m	900-999m	>999m	Cloud Entirely Transition	Total
1000		1									1	1	3
6000-7000	1	5	2		1								9
8000-10000	2	12	6	2		1						1	24
12000-14000		1		4	1								6
15000-16900	2	9	4	5	1								21
17100-18900	2	6	1	1									10
20000-21000		2	1	1				1					5
Total	7	35	15	13	3	1		1			1	2	78

TABLE 8. DISTRIBUTION OF TRANSITION ZONE SIZES THROUGH WHICH $\int \Delta N dS$ WAS COMPUTED

Cloud Type	0	<100m	100-199m	200-299m	300-399m	400-499m	500-599m	600-699m	700-799m	800-899m	900-999m	>999m	Clouds Entirely Transition	Total
Continental Clouds	3	13	11	8	3	1			1			1	2	43
Ocean Clouds	5	12	6	8	3				1	1		4	11	51

the size distributions of the zones through which $\int \Delta NdS$ was computed. Statistical tests performed on these distributions to inquire if zone sizes are significantly larger in one population than in the other are inconclusive.

In tables 9 and 10 we examine transition zone sizes with respect to 200 m. Statistical tests on these 2 x 2 tables show that there is no significant difference between continental clouds and ocean clouds as regards proportions of transition zone sizes greater than or less than 200 m. This applies to all of the transition zone measurements and to the sample of measurements through which the integral functions were computed. We may conclude then that in choosing the 200 m point to evaluate the integral we are not sampling transition zone air more often in the ocean clouds.

TABLE 9. DISTRIBUTION OF TRANSITION ZONE SIZES WITH RESPECT TO 200 m ALL DATA

	<200 meters	>200 meters	Total
Continental Clouds	57	19	76
Ocean Clouds	268	103	371
Total	325	122	447

TABLE 10. DISTRIBUTION OF TRANSITION ZONE SIZES WITH RESPECT TO 200 m ZONES THROUGH WHICH $\int \Delta NdS$ WAS COMPUTED

	<200 meters	>200 meters	Total
Continental Clouds	27	16	43
Ocean Clouds	23	28	51
Total	50	44	94

Table 11 summarizes the measurements of refractive index difference between cloud core and environment air, $N_c - N_1$ (fig. 28). The measurements in the distributions labeled "sample" apply to the clouds for which integral functions have been computed. The data in the "population" distributions represent all the gross refractive index cloud measurements of (1), of Section IV, and some made and reported by Cunningham (3).

The difference in sample means of $N_c - N_1$ is statistically significant, and is in the right direction to account for the difference in values of $(\int \Delta N dS)_{200}$ between continental and ocean clouds. The difference in population means is significant, but has a sign opposite to that of the difference in sample means. Further tests show the continental sample to be representative of the continental population but not so for the ocean sample and ocean population. The ocean sample of measurements of cloud-environment refractive index difference contains an unrepresentative proportion of small values.

Conclusions: We have measurements of the integrated cloud-environment refractive index difference along the flight path of the measuring aircraft. These measurements have been made in two cloud populations which may be considered meteorologically different: clouds over the sub-tropical ocean and clouds over the continental United States. The measurements show larger values of the integral function for continental clouds. These larger values of the integral may be accounted

for by larger values of cloud-environment refractive index difference associated with the continental clouds for which the integral functions were computed. A much larger mass of measurements of cloud environment refractive index difference from both cloud populations show a tendency for this statistic to be larger in the ocean clouds. Had we taken a larger sample of ocean clouds, or a more representative one, we should expect that the ocean clouds would produce larger values of the integral function.

It remains to explain the reason for the unrepresentativeness in our sample of ocean clouds. The greater frequency of larger values of cloud-environment refractive index difference in ocean clouds is generally attributable to the measurements made in the dry air above the tradewind inversion. The bulk of the cloud measurements for the computation of the integral function of the ocean clouds were made on data from the flight of 15 June 1956. Soundings onthis date (1) show relatively high humidities throughout, and measured values of cloud-environment refractive index difference on this flight were relatively low. This relatively non-typical day in the sub-tropics would seem to be leading us to spurious conclusions about comparative sizes of the integral function in continental clouds and clouds over the tropical oceans.

Table 12 offers the distribution of cloud sizes (length of flight path in cloud) for the clouds for which $\int \Delta N dS$ was computed. These

TABLE 11. DISTRIBUTION OF N_c-N_l. "SAMPLE" REFERS TO CLOUDS IN WHICH $\int \Delta NdS$ HAS BEEN COMPUTED. "POPULATION" REFERS TO ALL CLOUD MEASUREMENTS.

Clouds	0-4N	5-9N	10-14N	15-19N	20-24N	25-29N	30-34N	35-39N	40-44N	45-49N	50-54N	55-59N	Means N units
Continental													
Population	12	5(	49	19	5	1	6	4					12.1
Sample		14	17	4	2		4	1					14.0
Ocean													
Population	12	24	23	22	11	12	15	15	8	4	6	1	21.8
Sample	9	17	18	4		1							9.5

TABLE 12. DISTRIBUTION OF THE HORIZONTAL SIZES OF THE CLOUDS FOR WHICH $\int \Delta NdS$ WAS COMPUTED

	0-499m	500-999m	1000-1499m	1500-1999m	2000-2499m	2500-2999m	3000-3499m	3500-3999m	4000-4499m	4500-4999m	> 4999	Un-measure-able	Total
Continental	9	13	7	4	1	1					1	5	41
Ocean	14	12	7	1	5	1	1		1	2	3	5	52

sizes apply to single convective cells and are comparable to table 13, although here several cells may have come from one cloud.

TABLE 13. DISTRIBUTION OF CLOUD SIZES--SINGLE CELL

Size (meters)	Altitude in Feet															
	3000	3500	4000	5000	5500	6000	6500	7000	7500	8000	9000	10000	12000	13000	14000	Total
0 - 500	2		1			2	4	5	2	3					2	21
500 - 1000	1	2	2	3	2	2	1	1		1	2					17
1000 - 1500				3	2	4	2	1		2					1	15
1500 - 2000		1	1			1				2			1			6
2000 - 2500						1			1	1						3
2500 - 3000																
3000 - 3500						1										1
3500 - 4000				1		1										2

SECTION IV

MEASUREMENTS OF GROSS REFRACTIVE INDEX FEATURES OF CONVECTIVE CLOUDS

The foundation of the analysis of refractive index features of convective clouds is a model defined by the shape of the refractive index record trace as the aircraft passes from clear air through the cloud back into clear air. Fig. 28 presents schematically certain fundamental measurements based on this model. Cunningham (3) has provided summaries of these measurements for some continental clouds from his 1955 flights. In (1) the measurements for clouds over the Bahamas on 15 and 19 June 1956 were presented. In this section these measurements are offered for several of Cunningham's late 1956 flights in the Caribbean Area and also for two of his 1955 continental flights, the 17 July flight from Bedford to Wright Patterson Air Force Base and the 31 July flight west of Tucson.

The sizes of transition zones have been presented in tables 6 and 7.

Fig. 29 through 35 show for each cloud $N_c - N_1$, the difference between refractive index in the core of the cloud and refractive index at a point sufficiently remote from the cloud to be deemed representative of undisturbed environment air. Also presented in these figures is a curve representing the refractive index difference between an environment.

defined by radiosonde temperature and dew point, and saturated air at radiosonde temperature. The radiosonde ascents chosen were those nearest to the appropriate cloud areas in time and distance.

It is evident from these figures that the radiosonde and the aircraft do not necessarily sample the same refractive index atmosphere. The explanation for this which immediately comes to mind is the frequent remoteness of the cloud areas from the radiosonde station in both time and space. For example, clouds investigated in the Caribbean were compared with the San Juan sounding. The cloud areas were often as far as 200 miles from San Juan. In fig. 36, D, the difference between computed and measured environment-saturation refractive index difference is plotted against distance from the radiosonde station. These data include measurements from the late 1956 flights and from the flights of 15 and 19 June 1956. The distances are computed from the position reports in the aircraft navigator's log and are accurate only to several tens of miles. Nevertheless, it is evident that the size of D is not dependent upon the distance. A similar absence of a relationship between D and the time between the cloud measurement and sounding is demonstrated in fig. 37. It seems reasonable to suppose that the frequent lack of agreement between radiosonde and refractometer measurements to saturation-environment refractive index difference is merely a manifestation of the natural variability of water vapor in the atmosphere.

Tables 13 and 14 present the frequencies of cloud-size measurement with respect to the altitude of cloud penetration. All of the cloud size measurements for the flights of 20 November, 28 November, 30 November, 3 December, and 7 December are pooled. Table 13 includes only single cell clouds. Table 14 contains measurements for clouds which consisted of more than one cell or which had air within them exhibiting refractive index values approaching those of environment air.

Fig. 38 through 44 show N_2-N_1 for the clouds from five of the late 1956 flights and 2 of the 1955 flights. The measurements presented in these figures are the ones made at the inbound cloud face. N_2-N_1 is a measure of the modification of environment refractive index due to the presence of cloud. When converted to units of humidity, N_2-N_1 is an indication of the amount of environment moistening which a cloud may produce. When presented as they are here, the values of N_2-N_1 are distributed about a mean value of 0. This is because the aircraft headings on the cloud penetrations were fairly well randomized. It is not too difficult to demonstrate that there is a rather high correlation between the values of N_2-N_1 and the heading of the aircraft with respect to the direction of the shear vector which is acting upon the cloud at the altitude of measurement. An investigation of environment moistening based on these measurements of N_2-N_1 and its relationship to vertical wind shear is the basis of analysis to be considered in the second of these final reports.

TABLE 14. DISTRIBUTION OF CLOUD SIZES--MULTIPLE CELL

Size (meters)	3000	3500	4000	5000	5500	6000	6500	7000	7500	8000	9000	10000	12000	13000	14000	Total
0 - 500	1									2				1		4
500 - 1000				1		1	1	1	1	1						6
1000 - 1500						1	1	2				1				5
1500 - 2000					1	3	2				1	1				8
2000 - 2500		2				2					2					6
2500 - 3000	1			1		1										3
3000 - 3500						2			1	1			3			7
3500 - 4000								1								1
6700 - 7800								1								1

ACKNOWLEDGEMENTS

Dr. Robert M. Cunningham of Air Force Cambrdige Research Center provided the data for this study. He and Dr. Roscoe R. Braham of the University of Chicago participated in many helpful discussions of analysis problems with the author.

Messrs. R. Morton, P. Kneip, and F. Teren were responsible for evaluation of the data.

REFERENCES

1. Braham, R. R., Jr., and E. L. Harrington, 1958: Cloud refractive index studies. Part I: Gradient distributions. (Tech. Note No. 11, Cloud Physics Lab.) Chicago, Dept. of Meteor., Univ. of Chicago, 37 pp.

2. Braham, R. R., Jr., E. L. Harrington, and T. E. Hoffer, 1958: Cloud refractive index studies. Part II: Use of distribution of ΔN vs. ΔS for estimating mechanical turbulence. (Tech. Note No. 17, Cloud Physics Lab.) Chicago, Dept. of Meteor., Univ. of Chicago, 18 pp.

3. Cunningham, R. M., V. G. Plank, and C. F. Campen, 1956: Cloud refractive index studies. Geophysical Res. Paper #51, Geo. Res. Directorate, A. F. C. R. C.

4. Snedecor, G. W., Statistical methods applied to experiments in agriculture and biology. Iowa State College Press, Ames, Iowa, 523 pp.

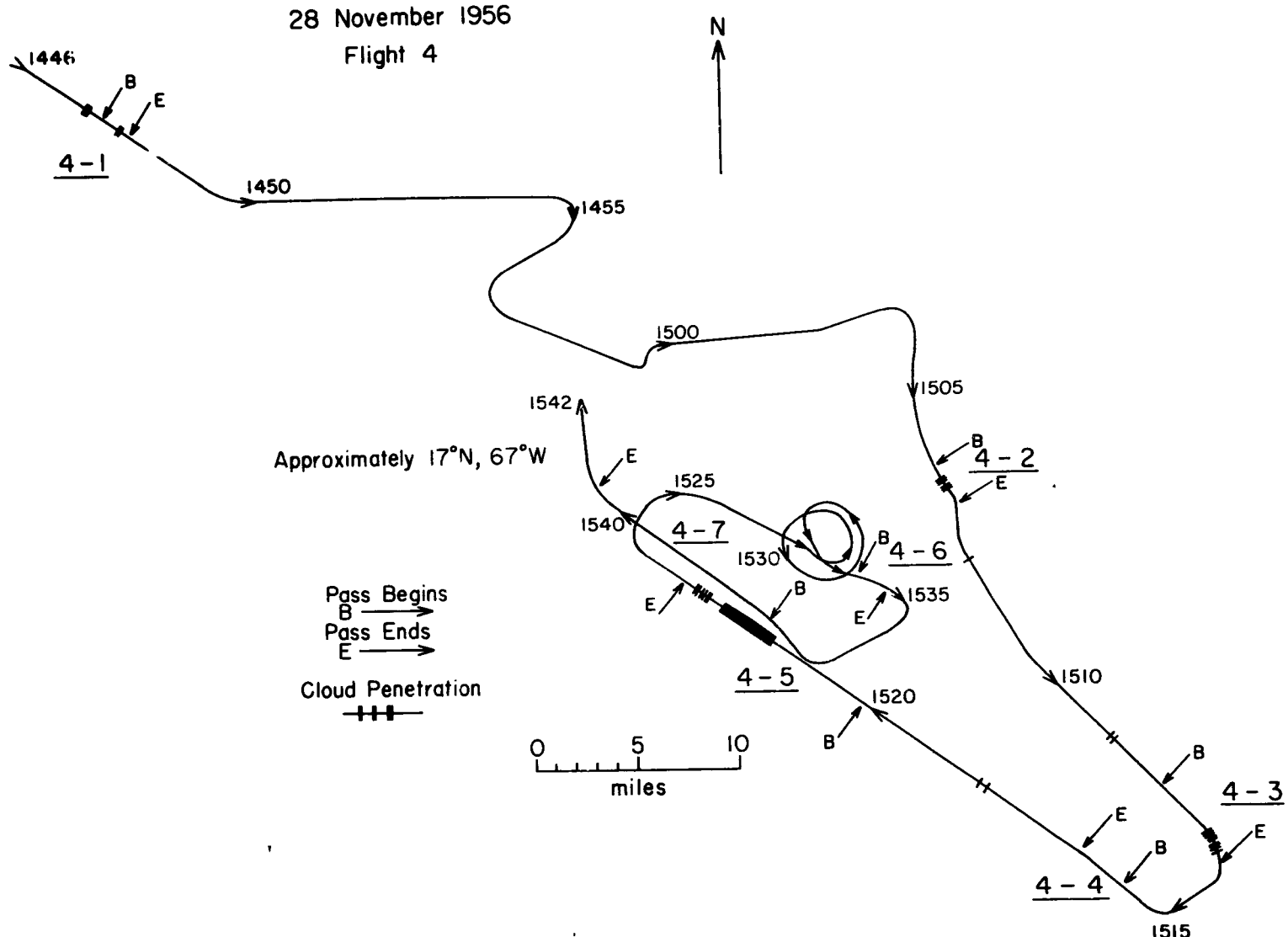

Fig. 1. Aircraft flight path during low altitude refractive index measurements, 28 November 1956.

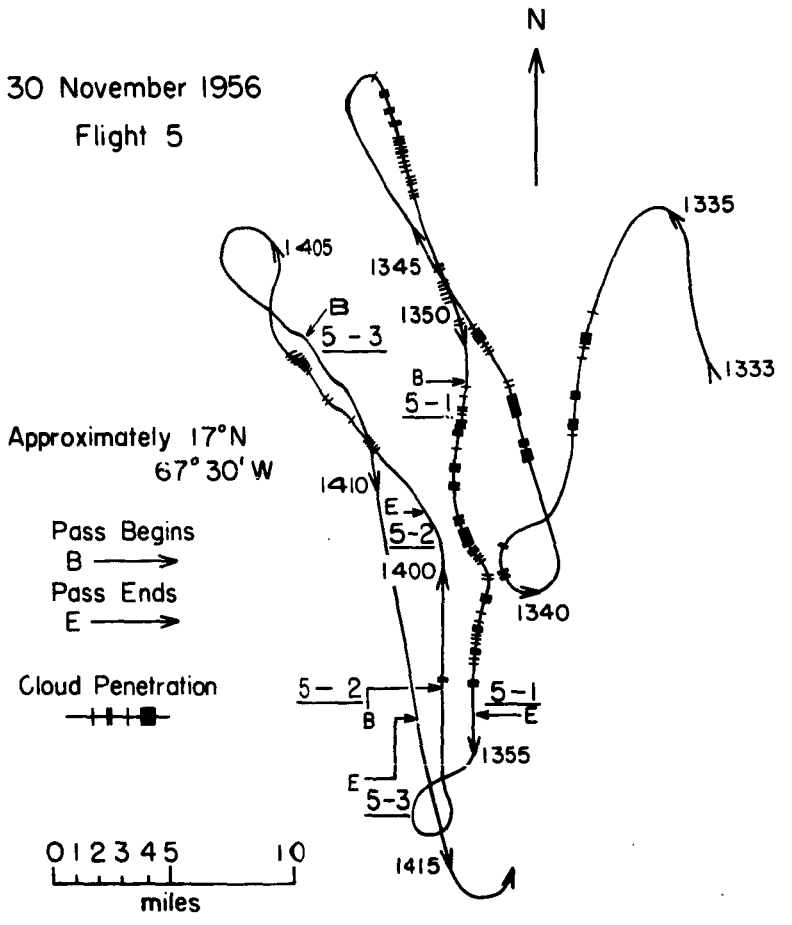

Fig. 2. Aircraft flight path during low altitude refractive index measurements, 30 November 1956.

Fig. 3 Low altitude pass 4-5 was made skimming the bases of these clouds.

Fig. 4 Low altitude pass 4-7 went below these clouds and passed through the shower area.

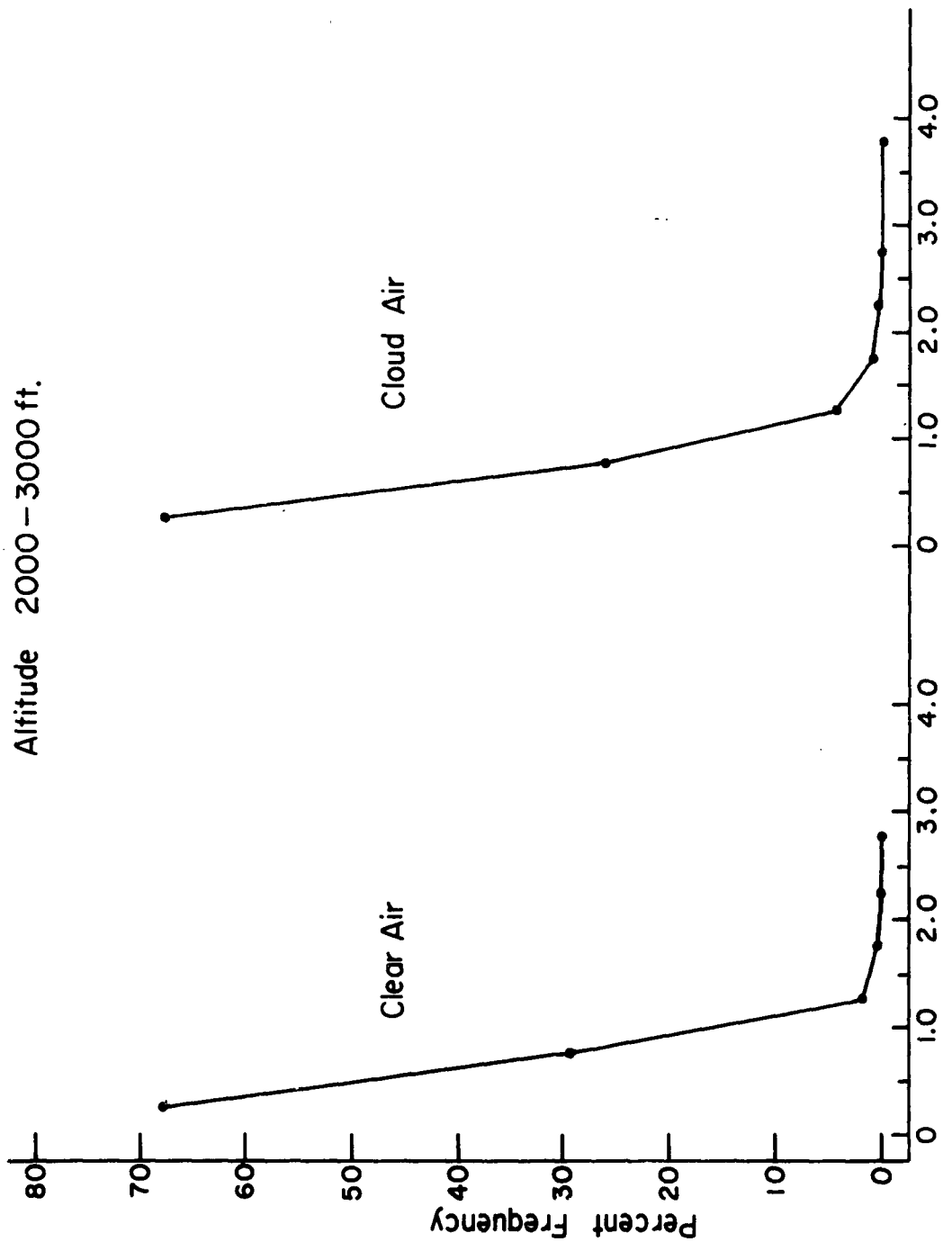

Fig. 5. Distributions of refractive index increments measured at altitudes from 2,000 to 3,000 ft.

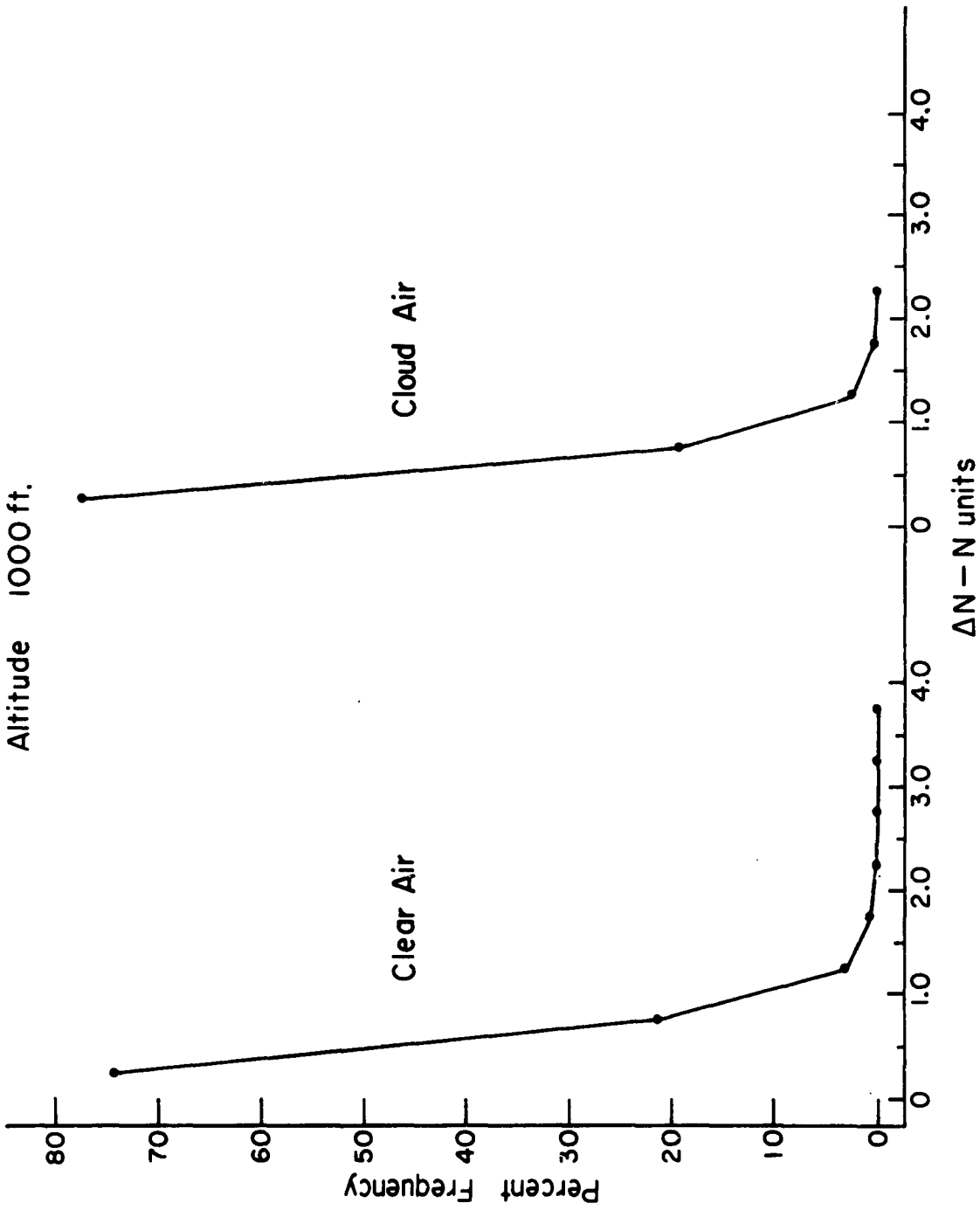

Fig. 6. Distributions of refractive index increments measured at 1,000 ft.

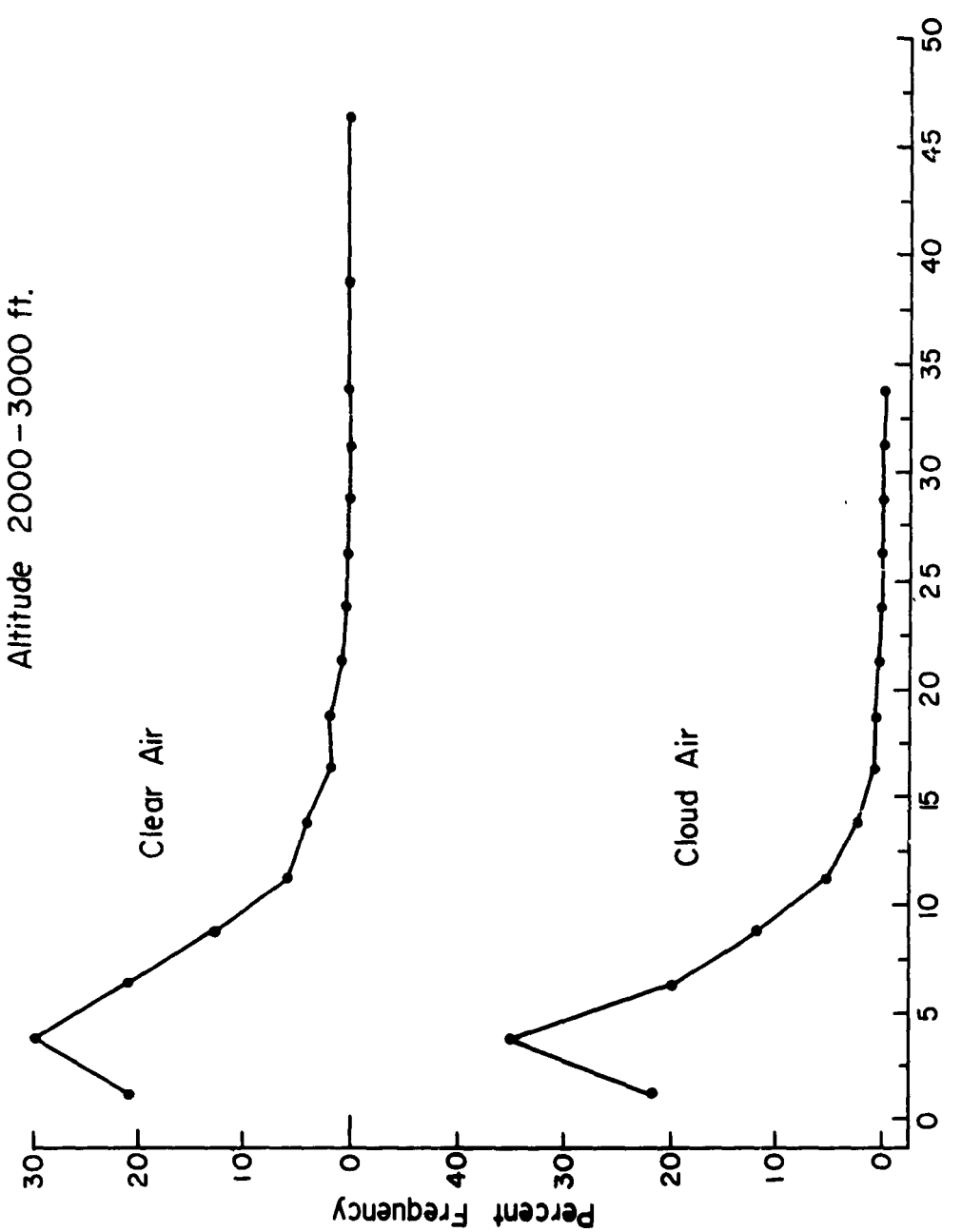

Fig. 7. Distributions of the sizes of path length over which refractive index increments were measured, altitude -- 2,000 to 3,000 ft.

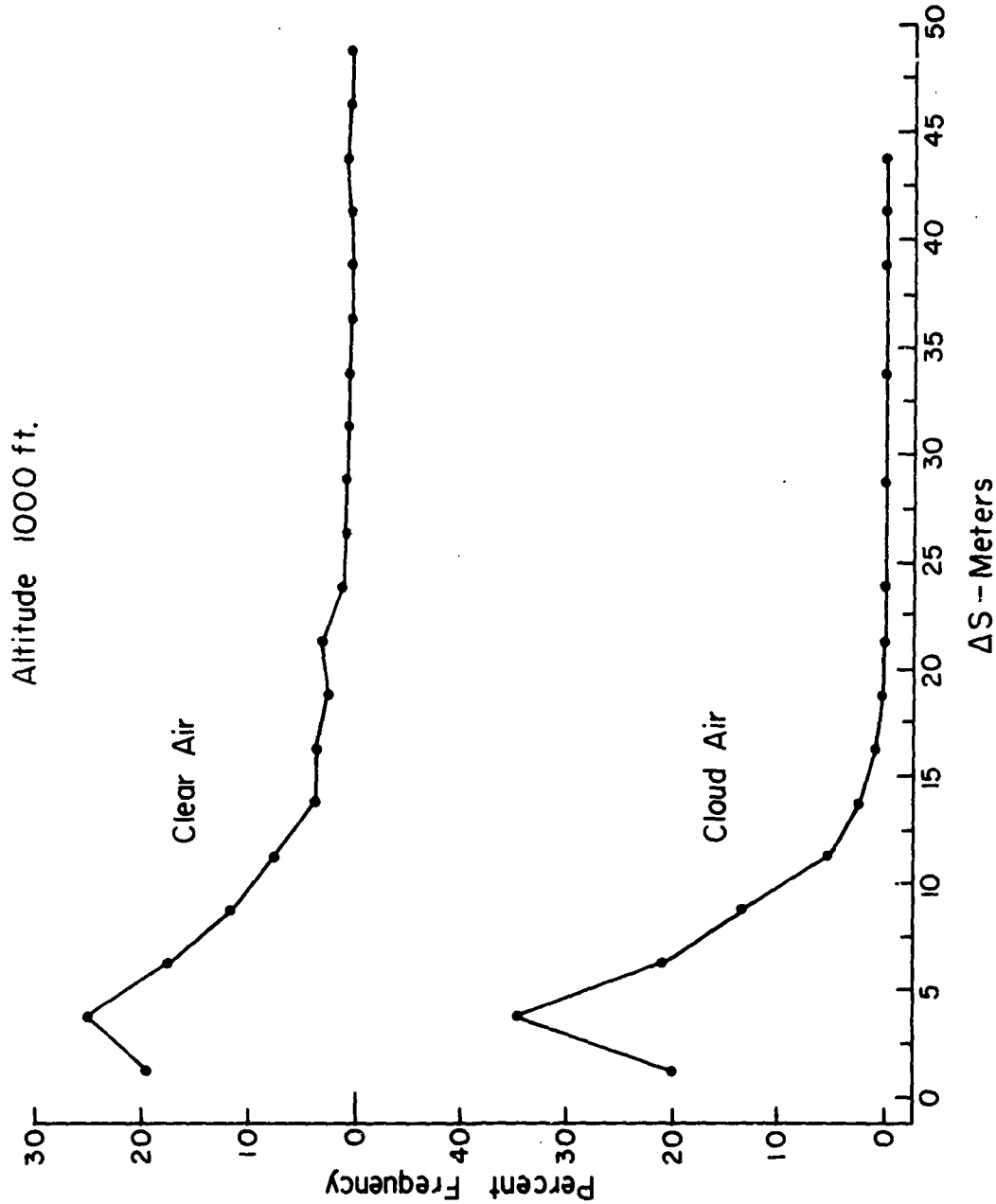

Fig. 8. Distributions of the sizes of path length over which refractive index increments were measured, altitude 1 000 ft

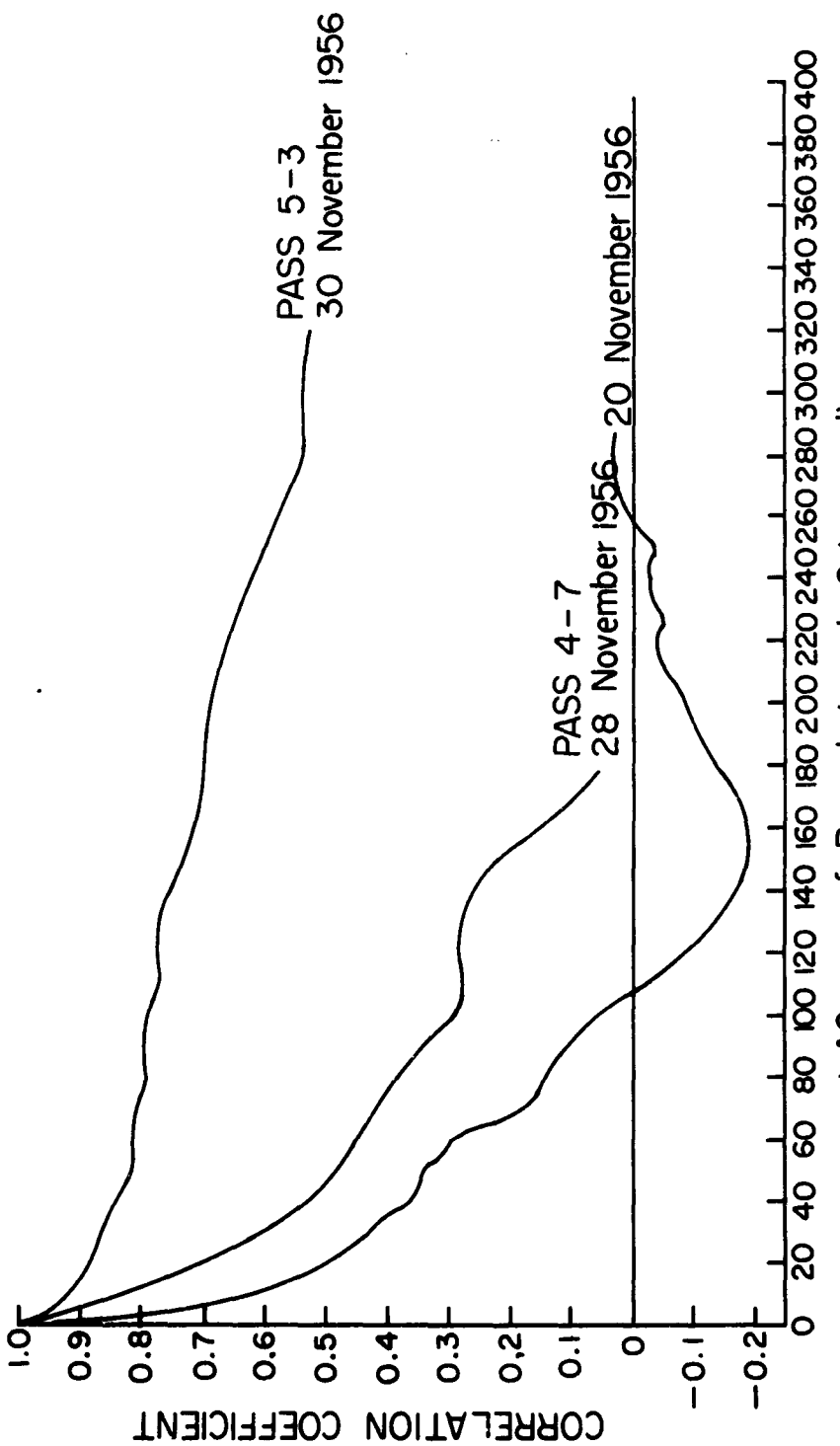

Fig. 9. Autocorrelation functions for three low altitude passes. The data record speed was 1 cm/sec. Data points were read at 1 mm intervals.

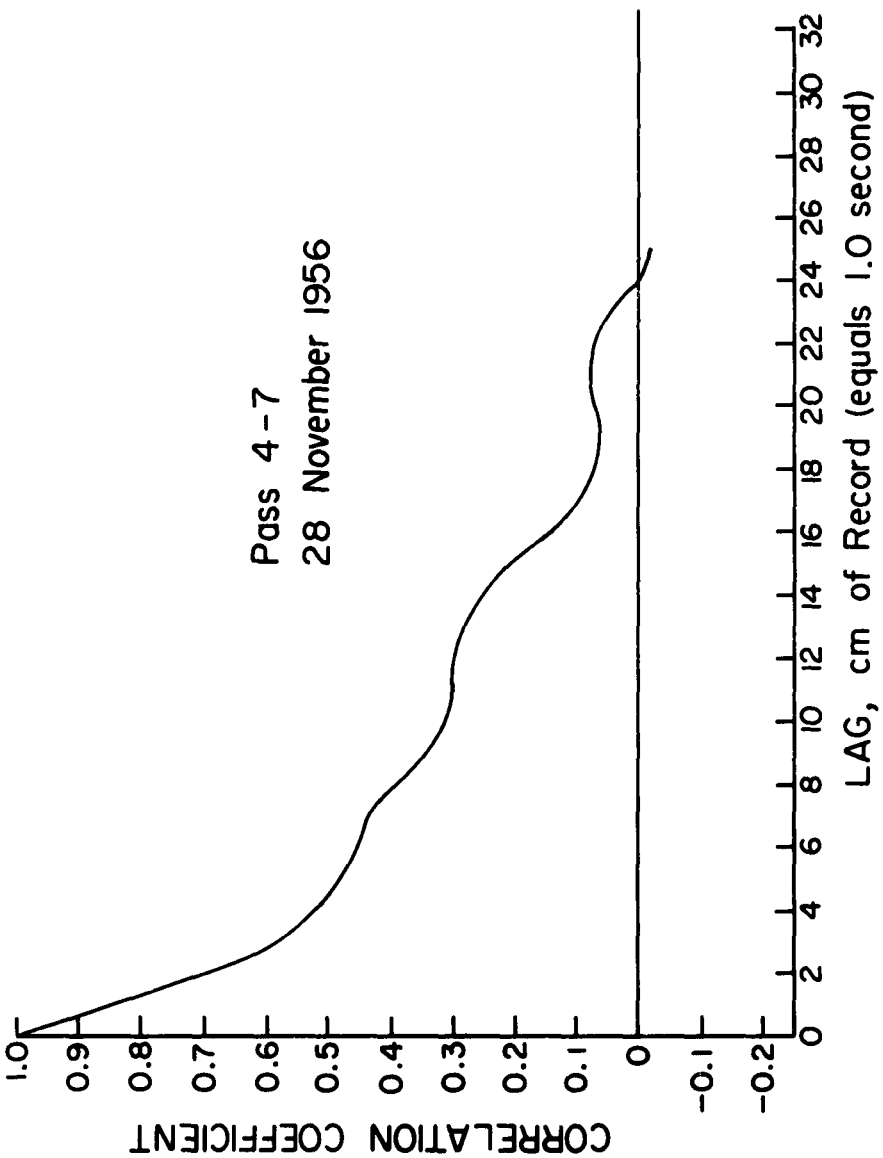

Fig. 10. Autocorrelation function for data points read at 1 cm intervals.

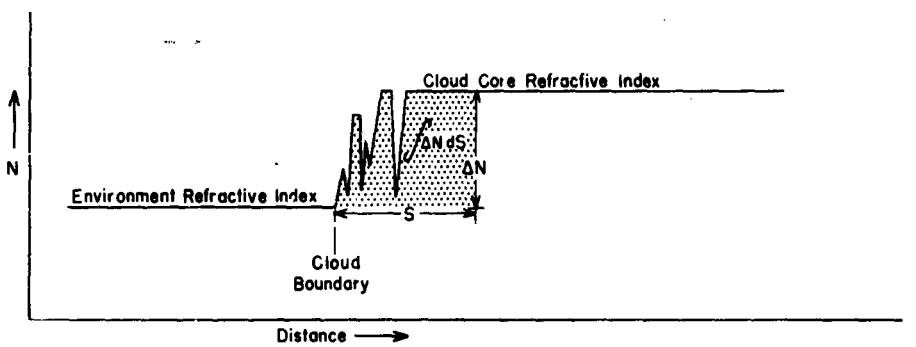

Fig. 11. $\int \Delta$ NdS with respect to a schematic refractive index record at the inbound cloud boundary.

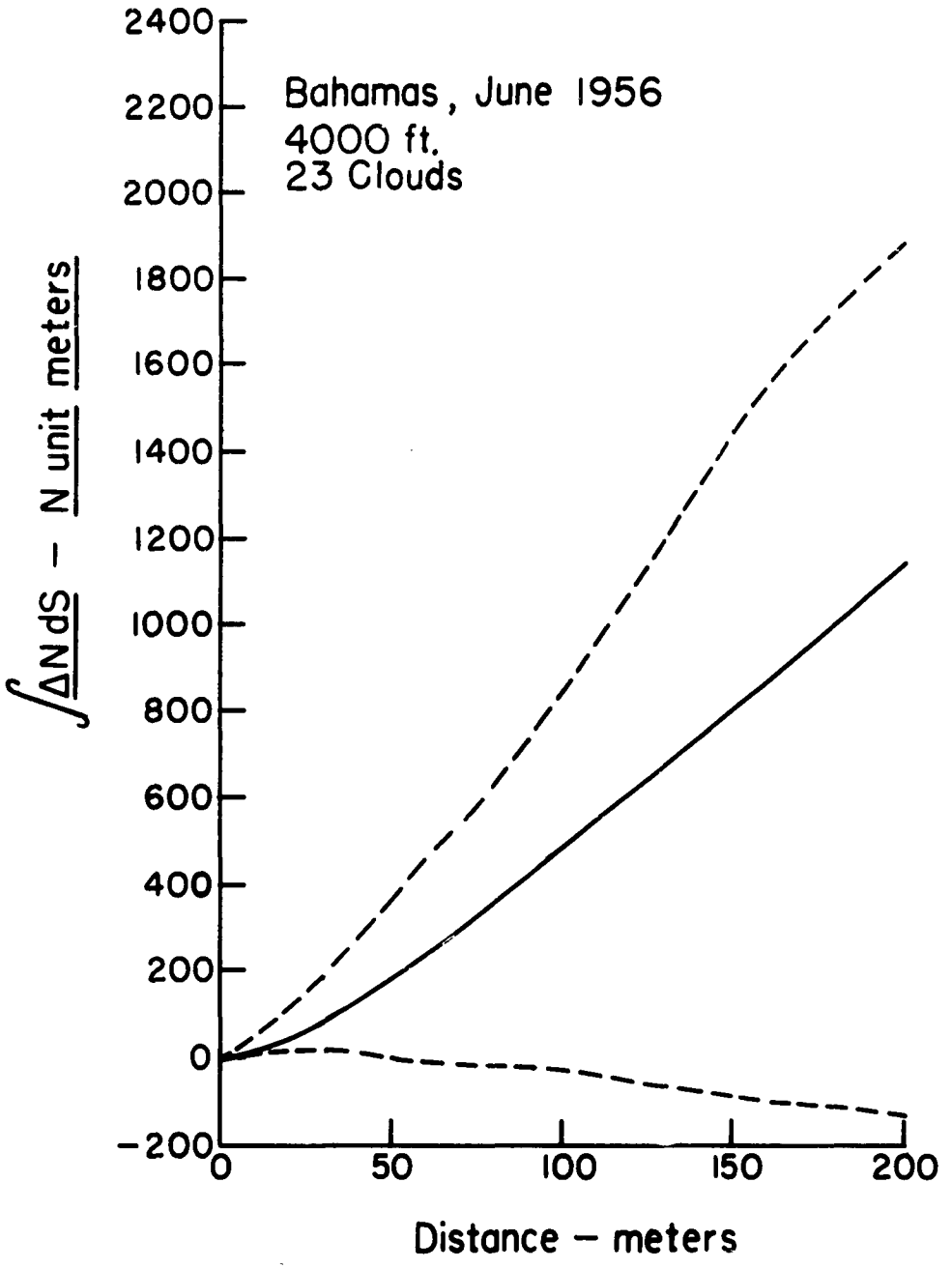
Bahamas, June 1956
4000 ft.
23 Clouds
∫ΔN dS - N unit meters
2400
2200
2000
1800
1600
1400
1200
1000
800
600
400
200
0
-200
0
50
100
150
200
Distance - meters

Fig. 12.

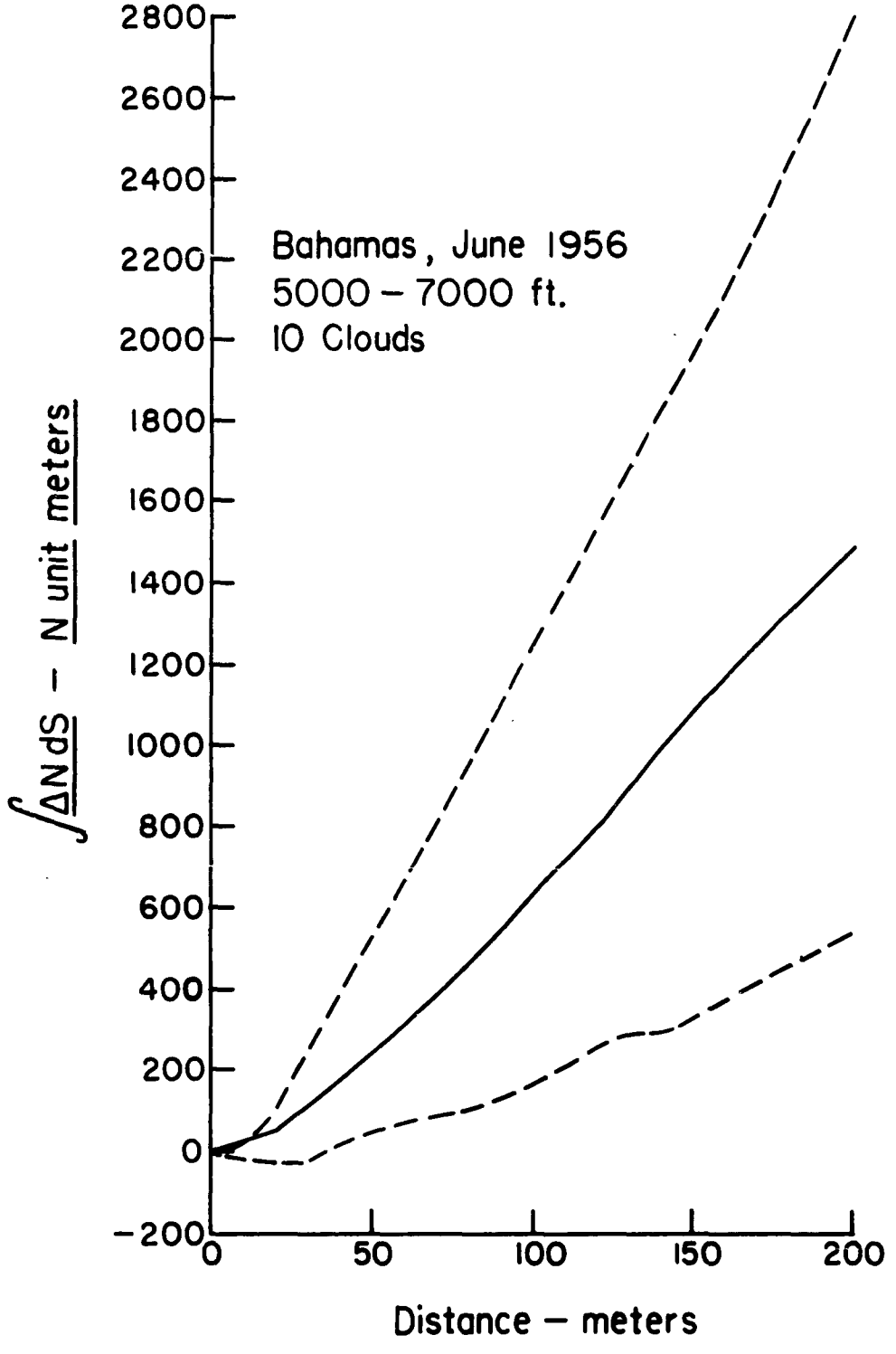
Bahamas, June 1956
5000 – 7000 ft.
10 Clouds
∫ΔN dS – N unit meters
2800
2600
2400
2200
2000
1800
1600
1400
1200
1000
800
600
400
200
0
-200
0
50
100
150
200
Distance – meters

Fig. 13.

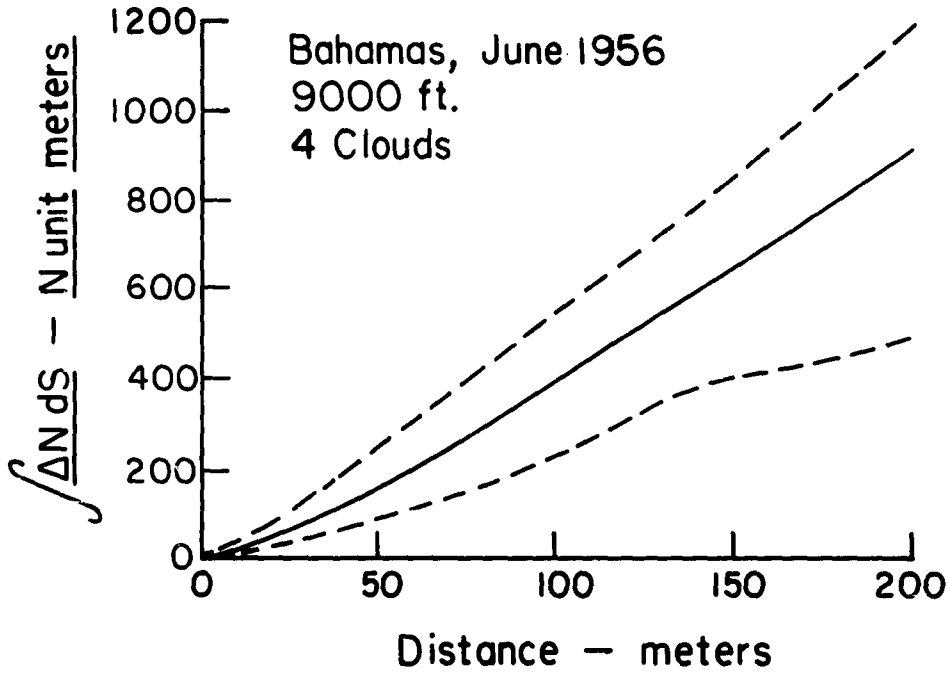
Bahamas, June 1956
9000 ft.
4 Clouds
∫ΔN dS - N unit meters
1200
1000
800
600
400
200
0
0
50
100
150
200
Distance — meters

Fig. 14.

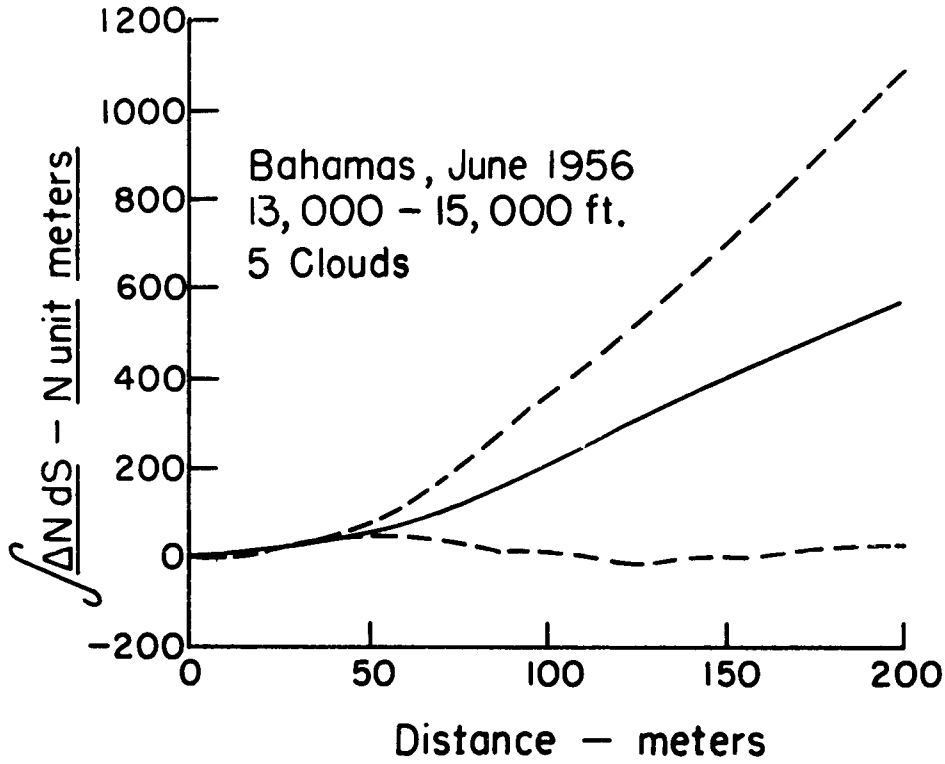
1200
1000
800
600
400
200
0
-200
0
50
100
150
200
Bahamas, June 1956
13,000 - 15,000 ft.
5 Clouds
∫ΔN dS - N unit meters
Distance — meters

Fig. 15.

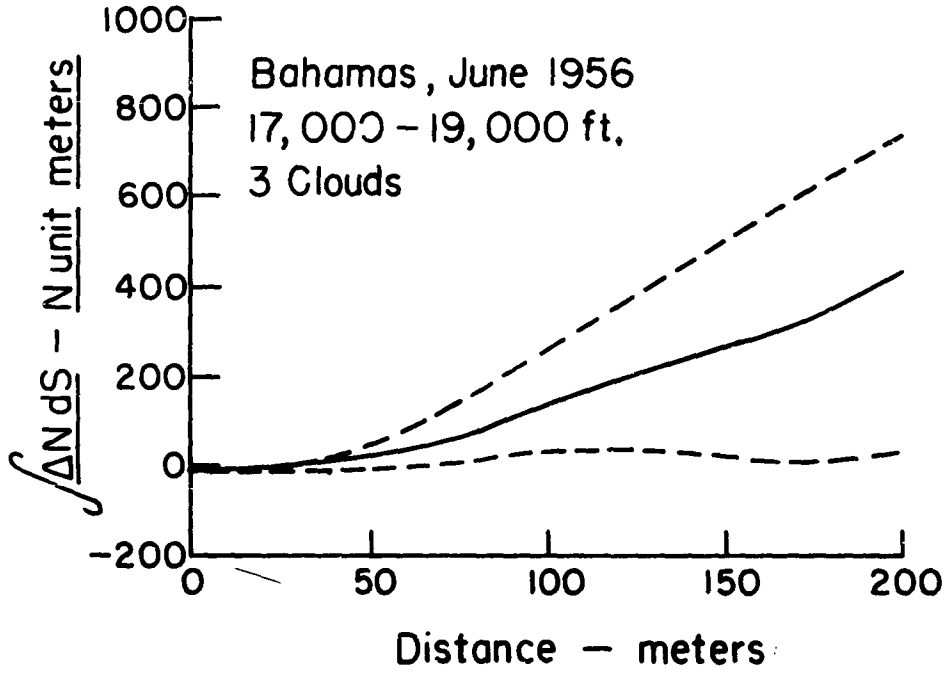
1000
800
600
400
200
0
-200
0
50
100
150
200
Bahamas, June 1956
17,000 - 19,000 ft.
3 Clouds
∫ΔN dS - N unit meters
Distance — meters

Fig. 16.

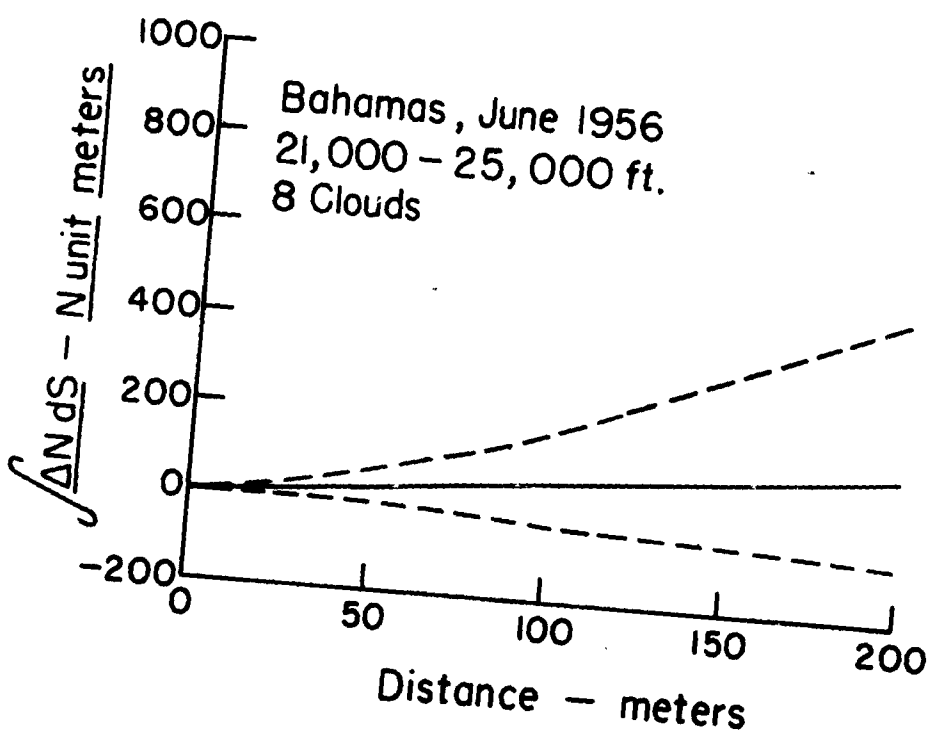
1000
800
600
400
200
0
-200
0
50
100
150
200
Bahamas, June 1956
21,000 – 25,000 ft.
8 Clouds
∫ΔN dS – N unit meters
Distance – meters

Fig. 17.

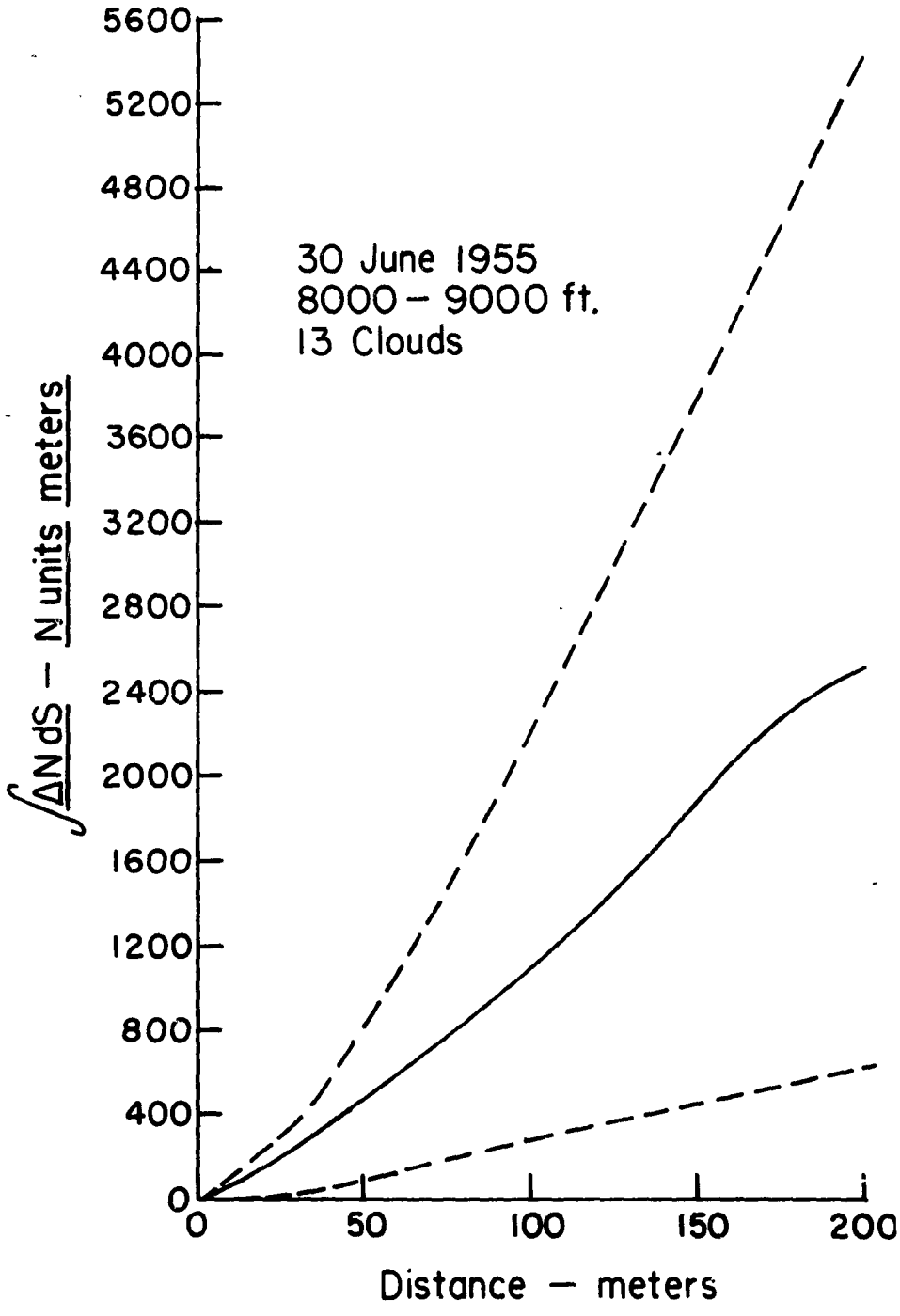
5600
5200
4800
4400
4000
3600
3200
2800
2400
2000
1600
1200
800
400
0
30 June 1955
8000 – 9000 ft.
13 Clouds
∫ΔN dS – N units meters
0
50
100
150
200
Distance – meters

Fig. 18.

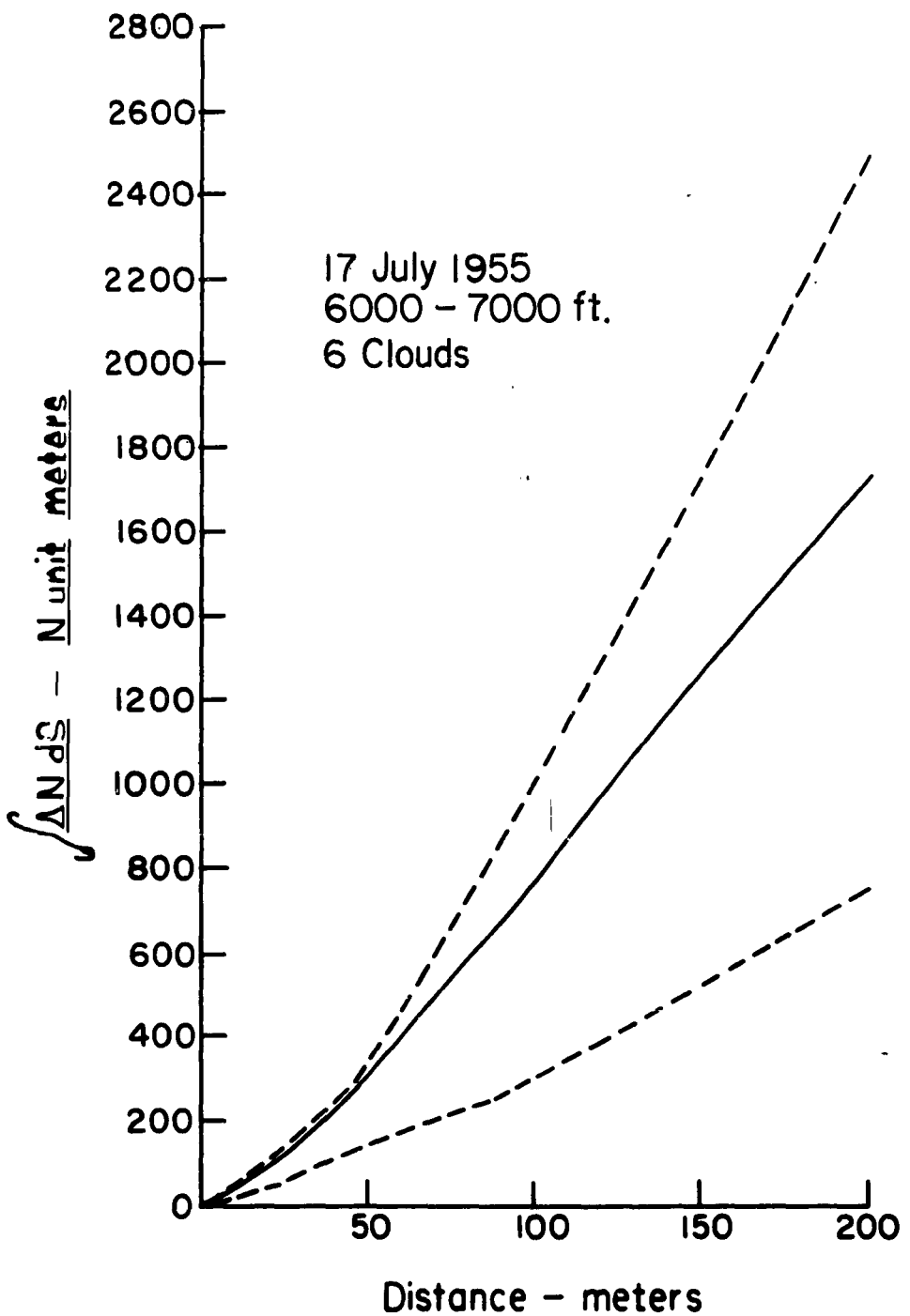
2800
2600
2400
2200
2000
1800
1600
1400
1200
1000
800
600
400
200
0
17 July 1955
6000 – 7000 ft.
6 Clouds
∫ΔN dS – N unit meters
50
100
150
200
Distance – meters

Fig. 19.

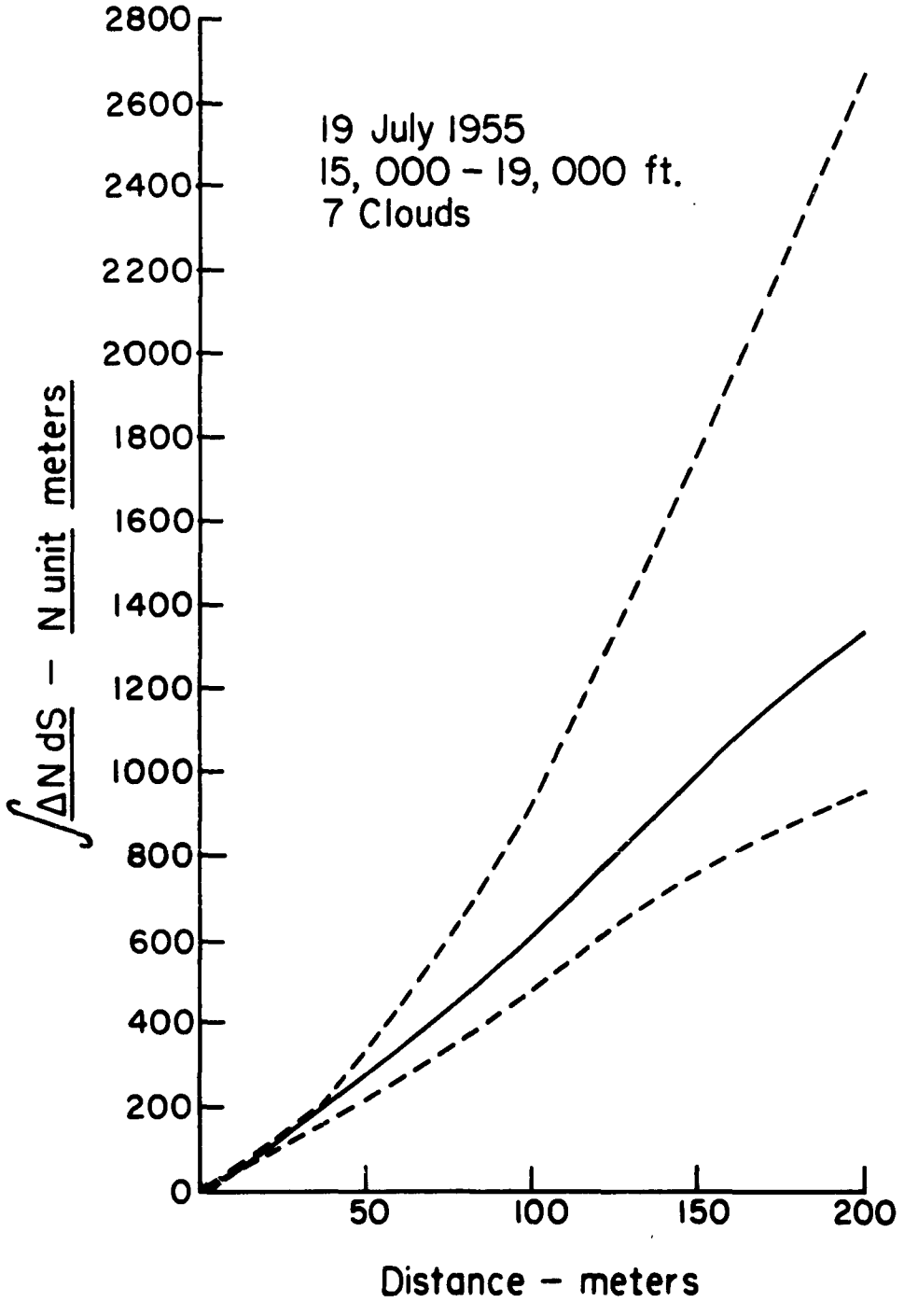
19 July 1955
15, 000 - 19, 000 ft.
7 Clouds
2800
2600
2400
2200
2000
1800
1600
1400
1200
1000
800
600
400
200
0
50
100
150
200
∫ΔN dS - N unit meters
Distance - meters

Fig. 20.

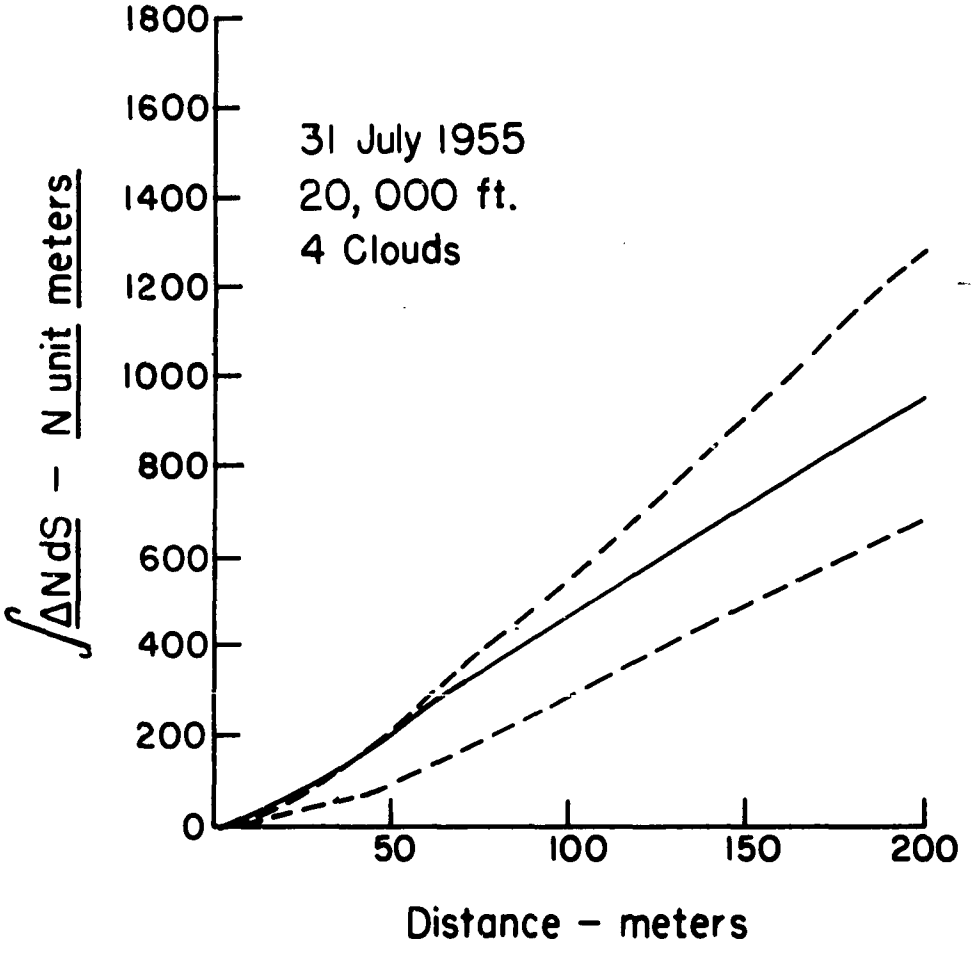
1800
1600
1400
1200
1000
800
600
400
200
0
50
100
150
200
31 July 1955
20, 000 ft.
4 Clouds
∫ΔN dS - N unit meters
Distance - meters

Fig. 21.

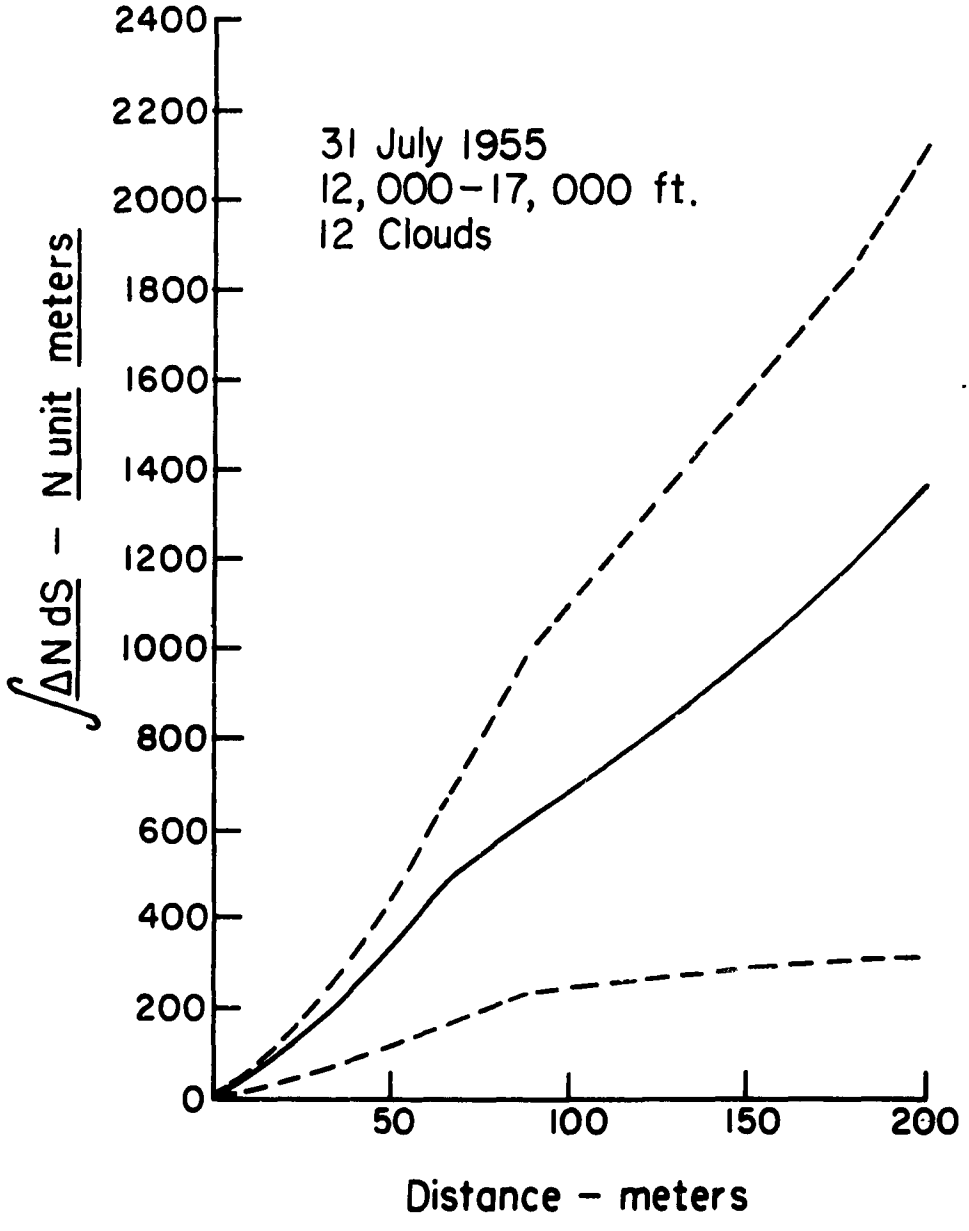
2400
2200
2000
1800
1600
1400
1200
1000
800
600
400
200
0
31 July 1955
12, 000-17, 000 ft.
12 Clouds
∫ΔN dS - N unit meters
50
100
150
200
Distance - meters

Fig. 22.

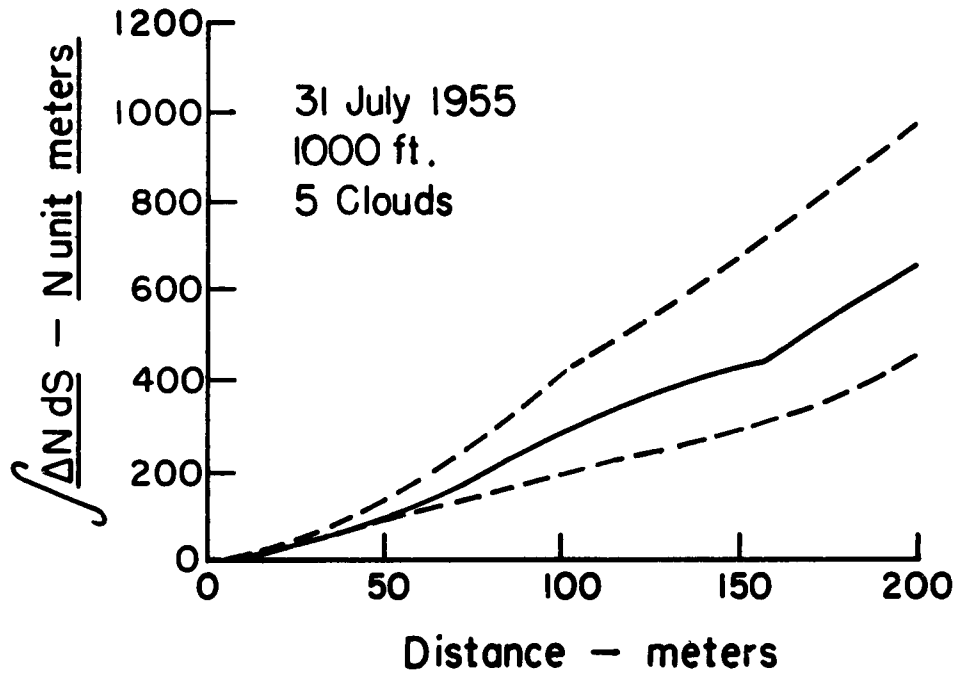
1200
1000
800
600
400
200
0
0
50
100
150
200
31 July 1955
1000 ft.
5 Clouds
∫ΔN dS – N unit meters
Distance – meters

Fig. 23.

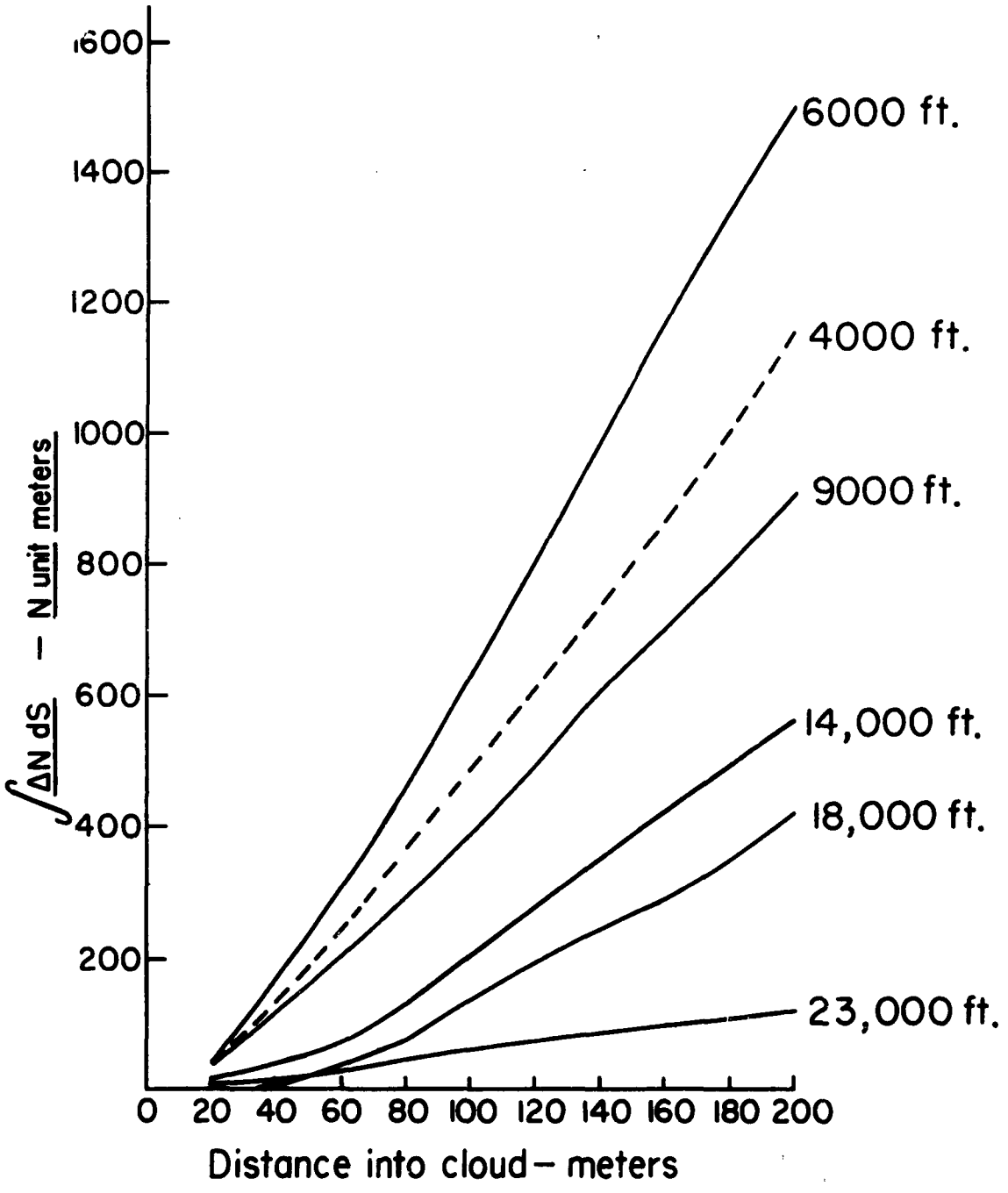

Fig. 24. Mean values of the integral function for selected altitudes.

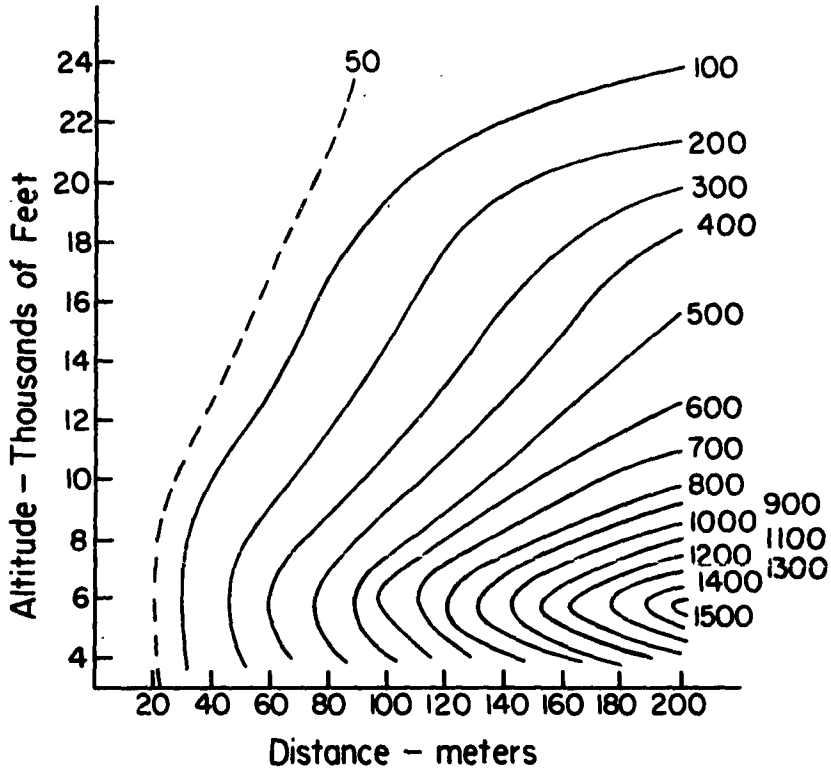

Fig. 25. Isopleths of the mean value of $\int \Delta NdS$, in N unit meters, for first 200 m of cloud.

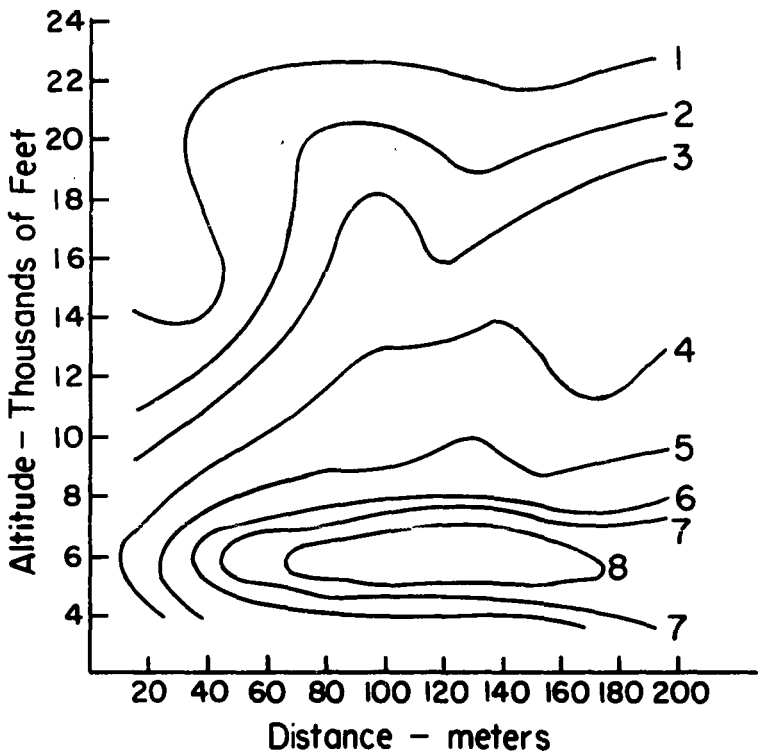

Fig. 26. Isopleths of the mean value of $\frac{d}{dS}\int \Delta NdS$ in N units, for first 200 m of cloud.

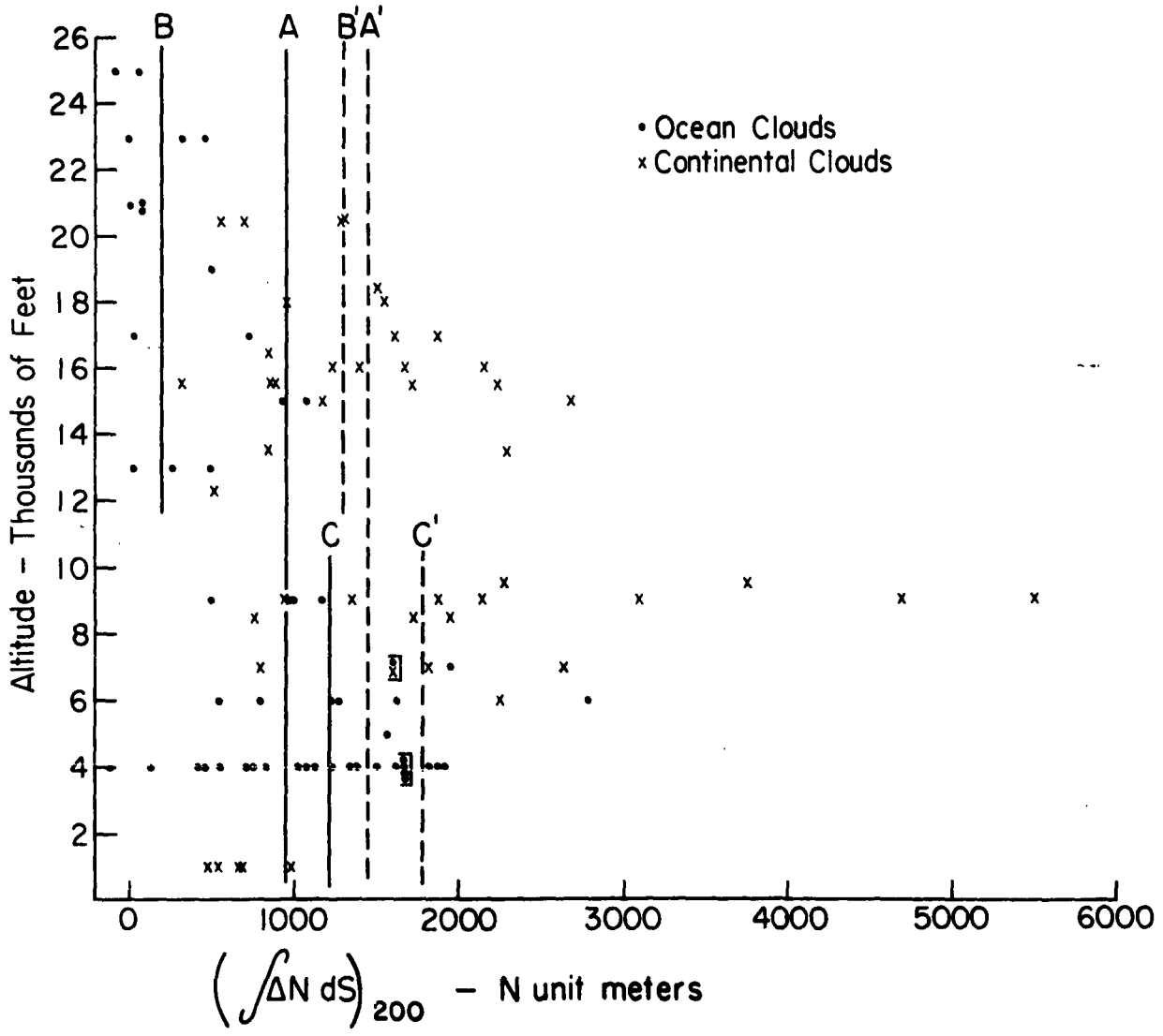

Fig. 27.

Values of the integral function at a point in the cloud 200 m from the cloud boundary. Vertical lines show median values: medians A, B and C apply to ocean clouds; A', B' and C' to continental clouds. Medians B and B' apply to the measurements above 12,000 ft., C and C' to the measurements below 12,000 ft., and A and A' to all measurements.

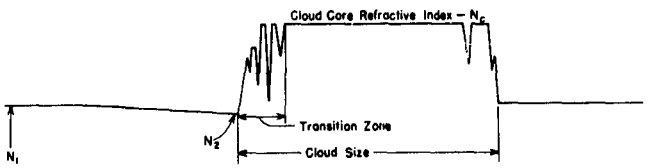

Fig. 28. Schematic representation of refractometer record for a cloud penetration, to demonstrate gross cloud refractive index measurements: N_c-N_1, the core-environment refractive index difference; N_2-N_1, environment refractive index change approaching the cloud; transition zone size; cloud size. N_1 is measured at least 15 sec prior to cloud entry.

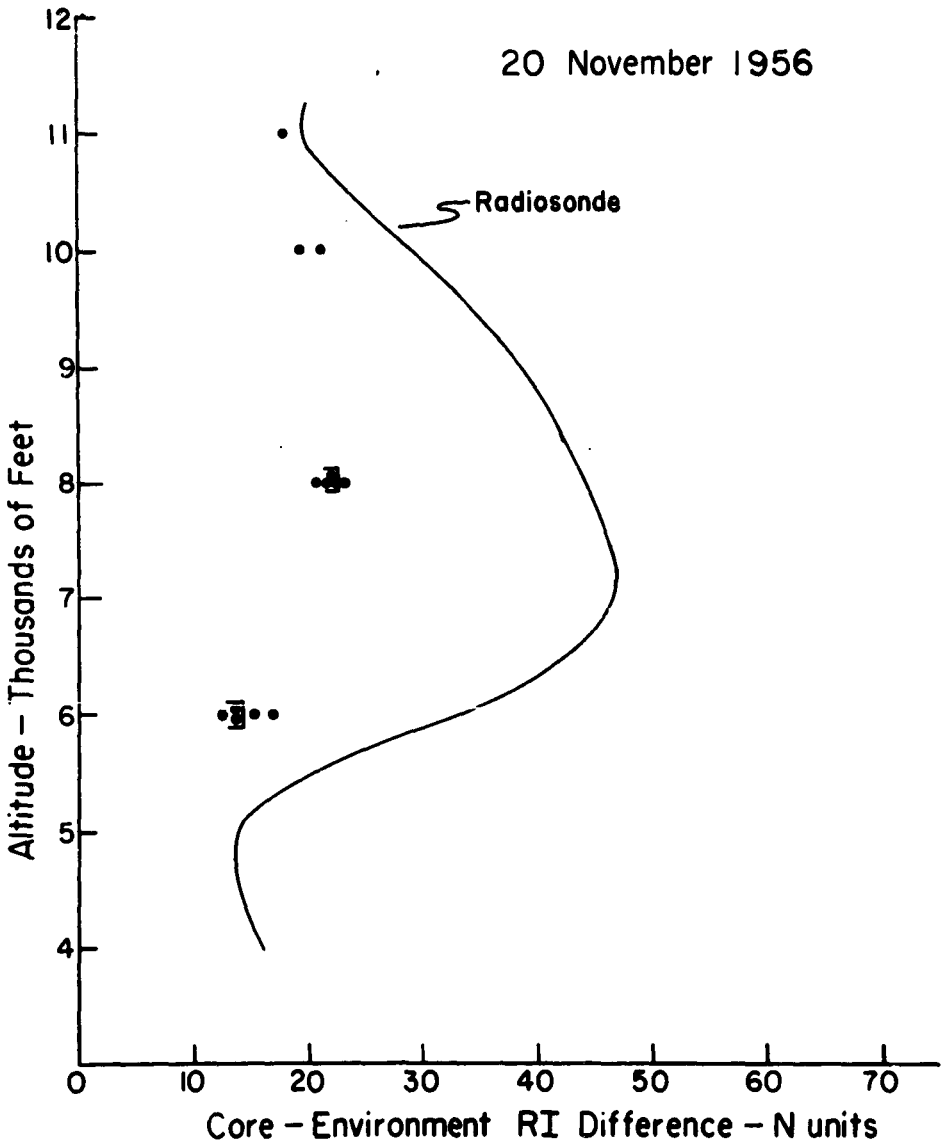
20 November 1956
Radiosonde
Altitude – Thousands of Feet
12
11
10
9
8
7
6
5
4
0
10
20
30
40
50
60
70
Core – Environment RI Difference – N units

Fig. 29.

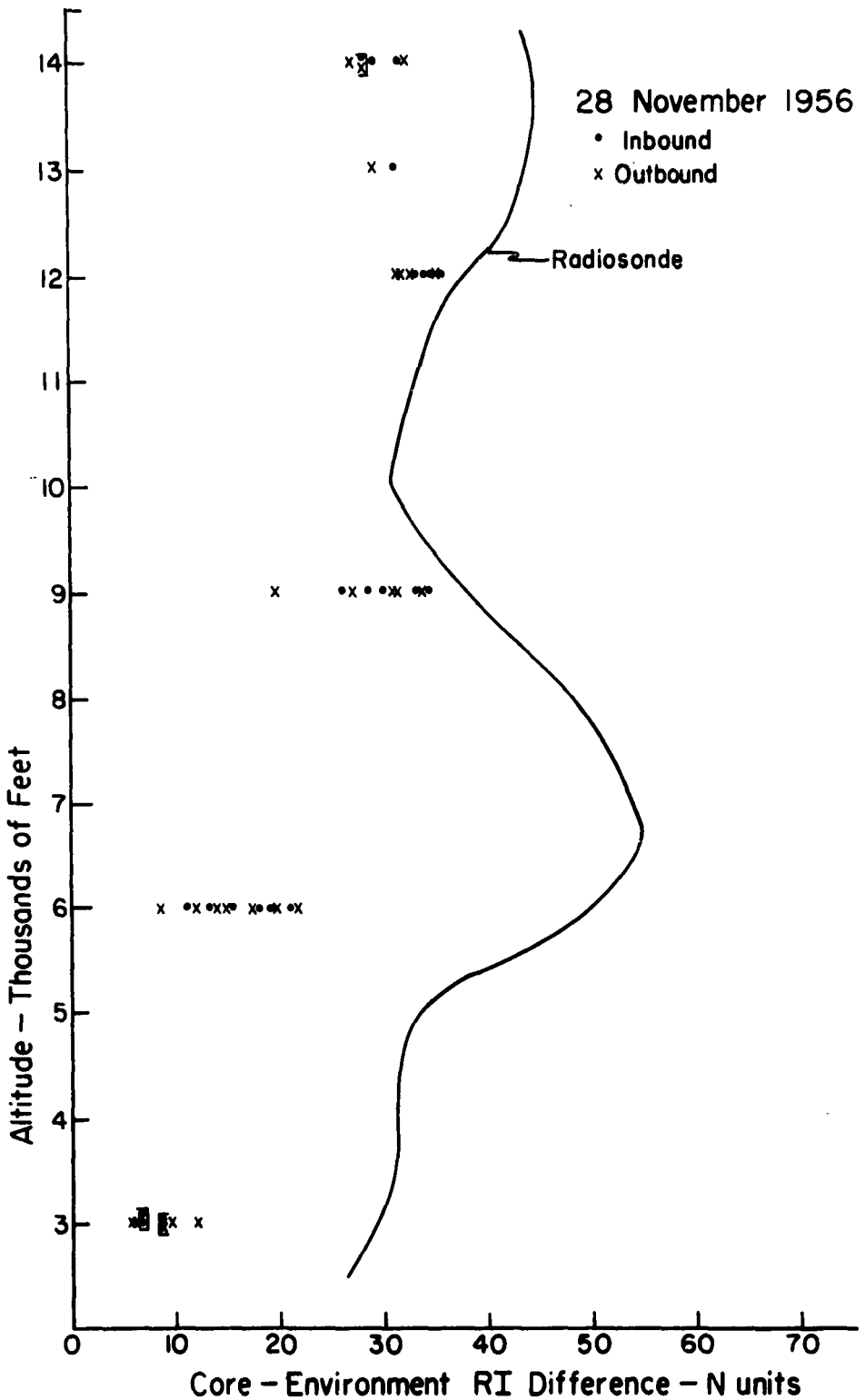
28 November 1956
• Inbound
x Outbound
Radiosonde
Altitude – Thousands of Feet
Core – Environment RI Difference – N units
14
13
12
11
10
9
8
7
6
5
4
3
0
10
20
30
40
50
60
70

Fig. 30.

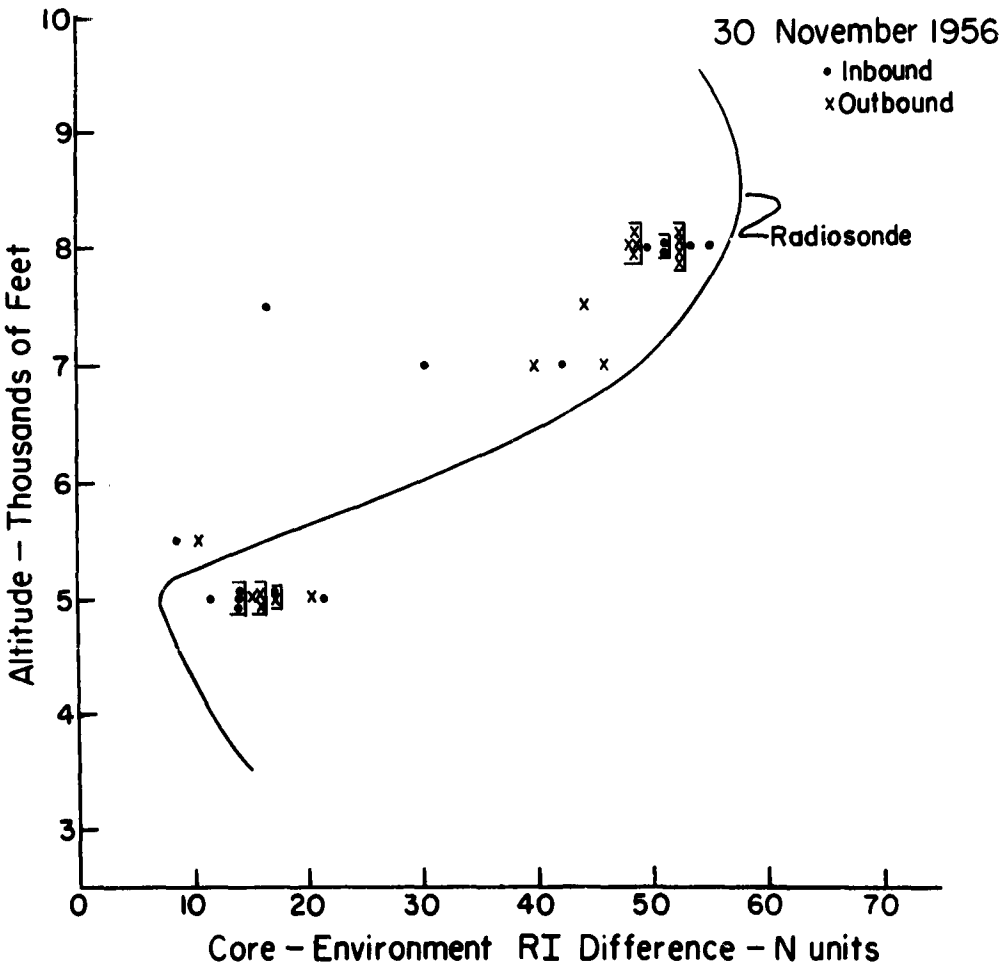
30 November 1956
• Inbound
x Outbound
Radiosonde
Altitude – Thousands of Feet
10
9
8
7
6
5
4
3
0
10
20
30
40
50
60
70
Core – Environment RI Difference – N units

Fig. 31.

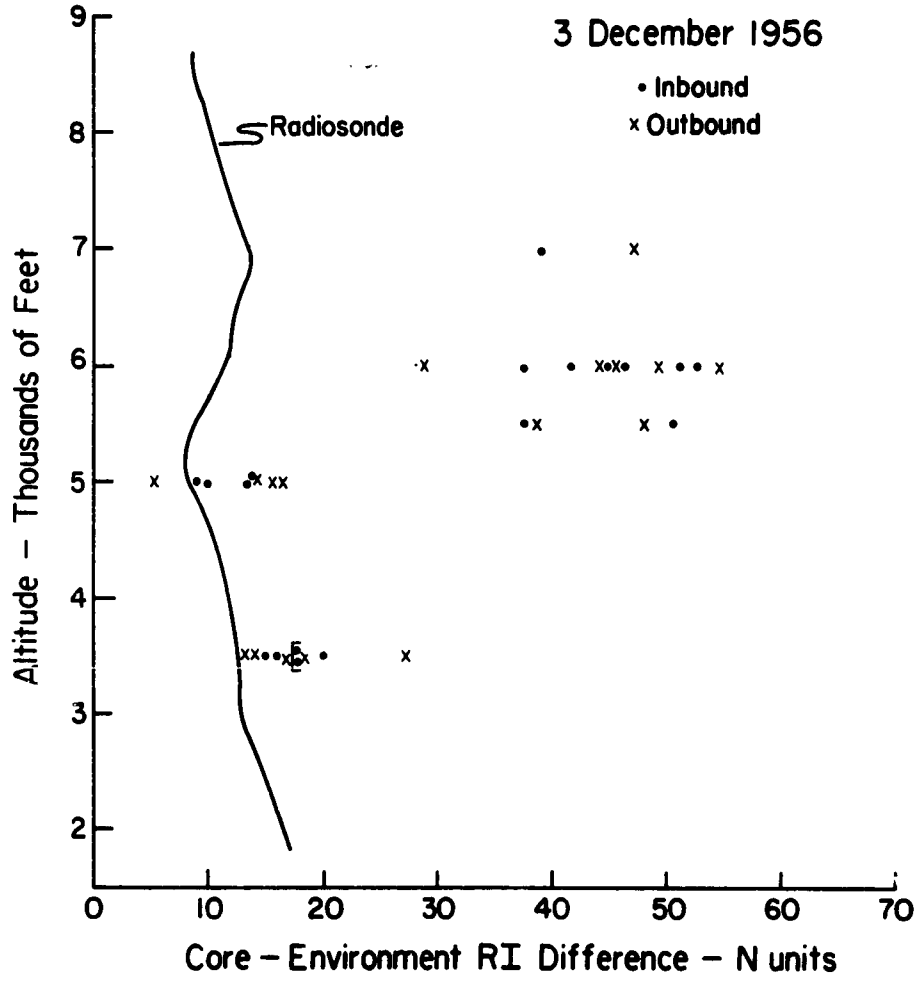
3 December 1956
• Inbound
x Outbound
Radiosonde
Altitude – Thousands of Feet
9
8
7
6
5
4
3
2
0
10
20
30
40
50
60
70
Core – Environment RI Difference – N units

Fig. 32.

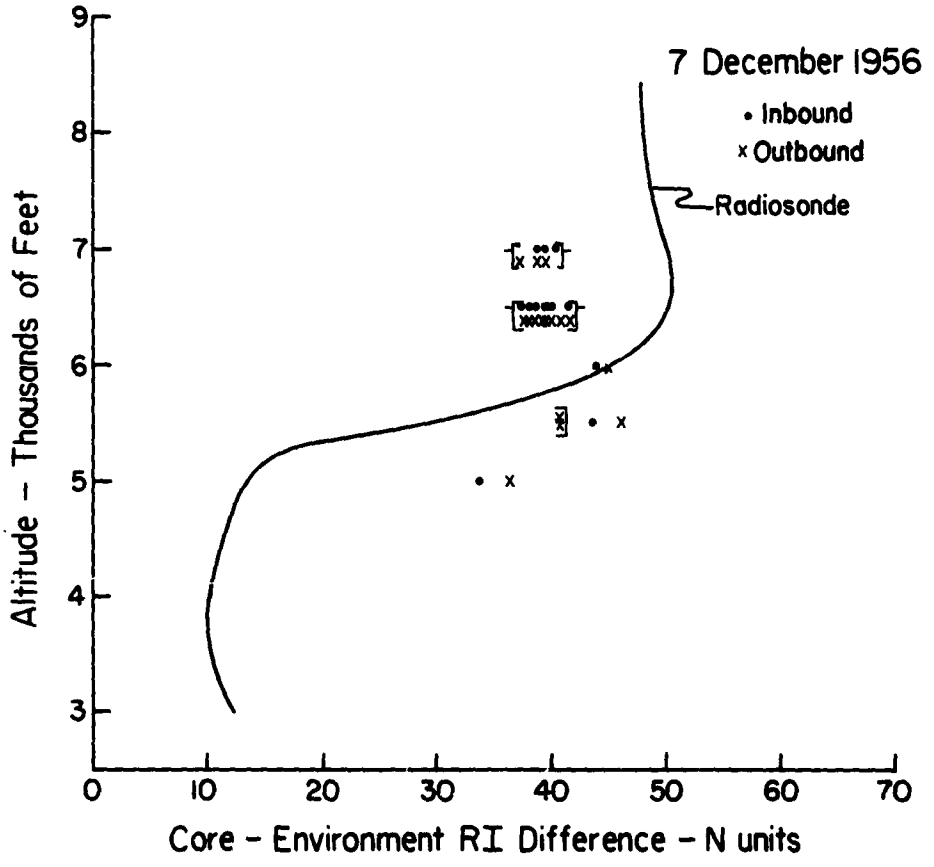
7 December 1956
• Inbound
x Outbound
Radiosonde
Altitude – Thousands of Feet
9
8
7
6
5
4
3
0
10
20
30
40
50
60
70
Core – Environment RI Difference – N units

Fig. 33.

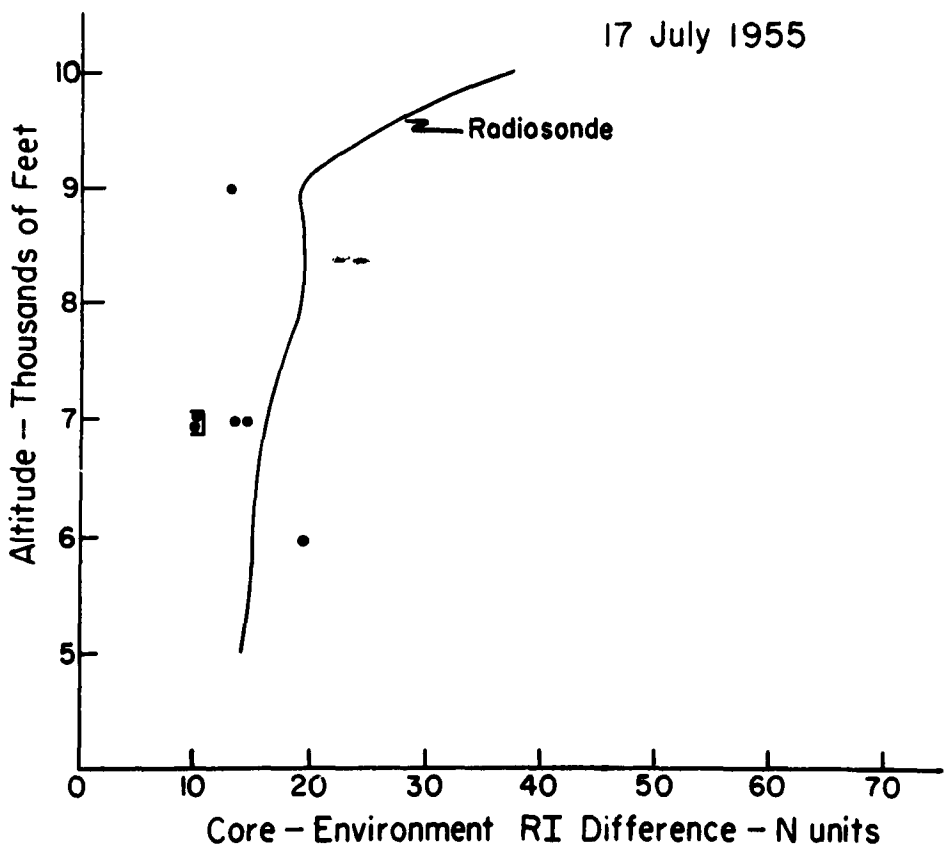
17 July 1955
Radiosonde
Altitude – Thousands of Feet
10
9
8
7
6
5
0
10
20
30
40
50
60
70
Core – Environment RI Difference – N units

Fig. 34.

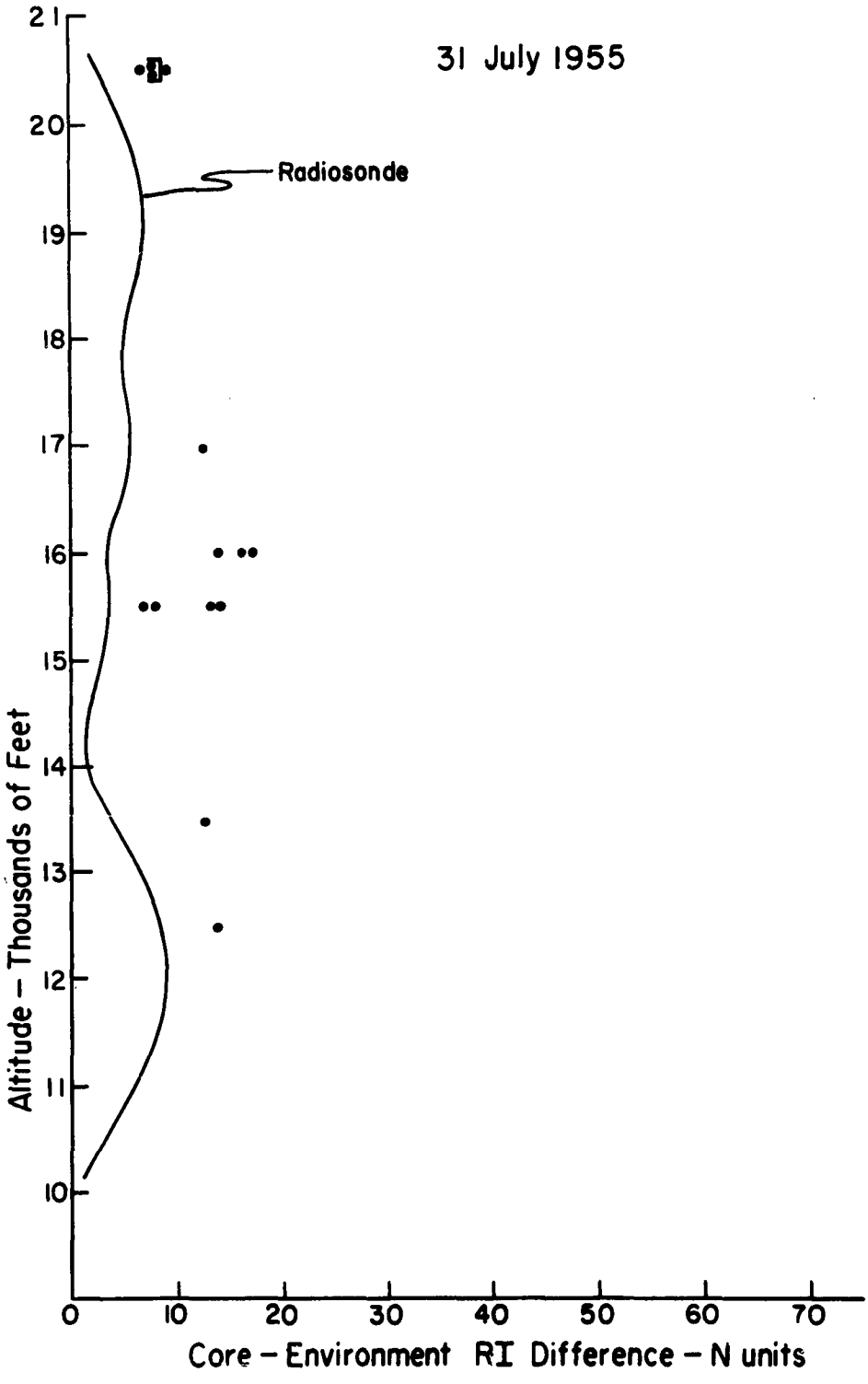
31 July 1955
Radiosonde
Altitude – Thousands of Feet
21
20
19
18
17
16
15
14
13
12
11
10
0
10
20
30
40
50
60
70
Core – Environment RI Difference – N units

Fig. 35.

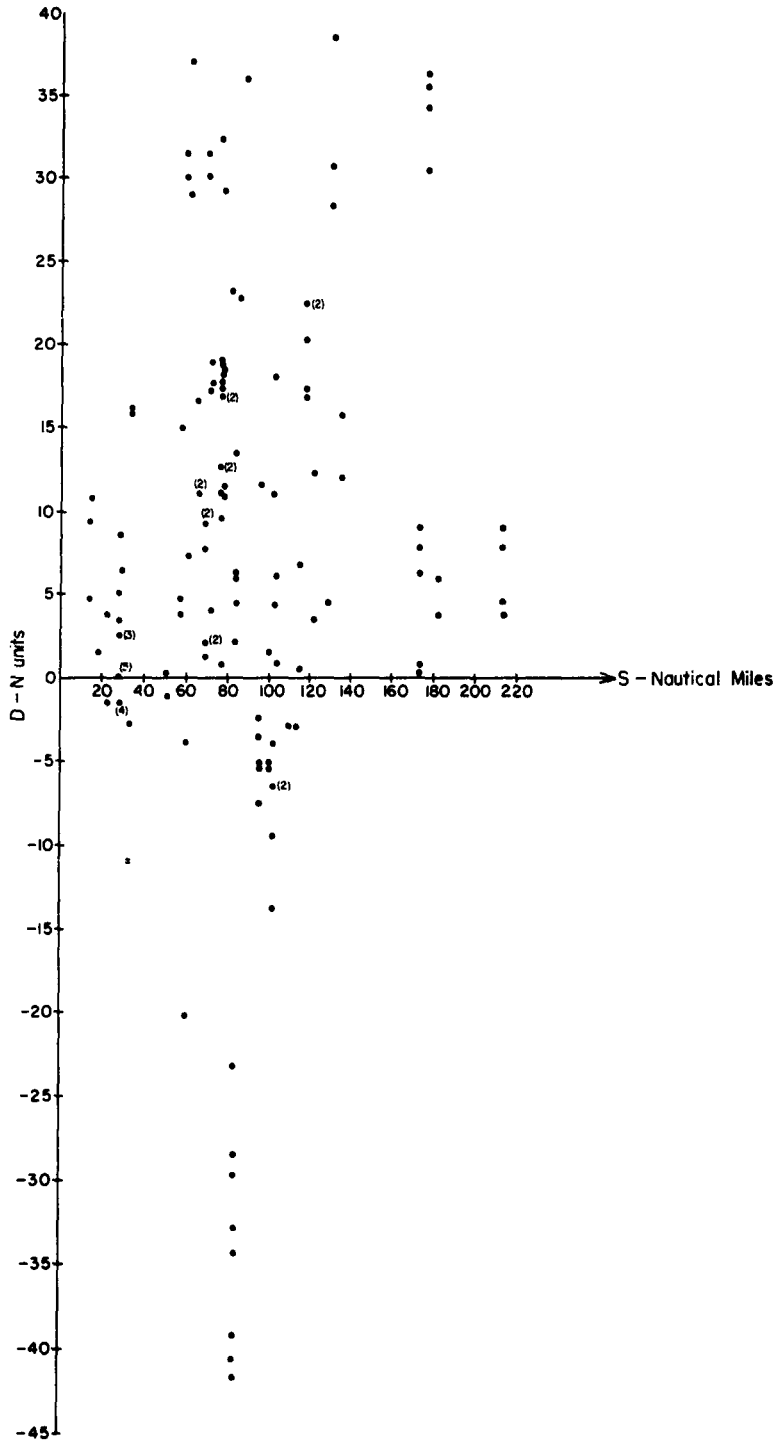

Fig. 36. D, the radiosonde saturation--environment refractive index difference minus measured value of core-environment refractive index difference, versus distance from the radiosonde station.

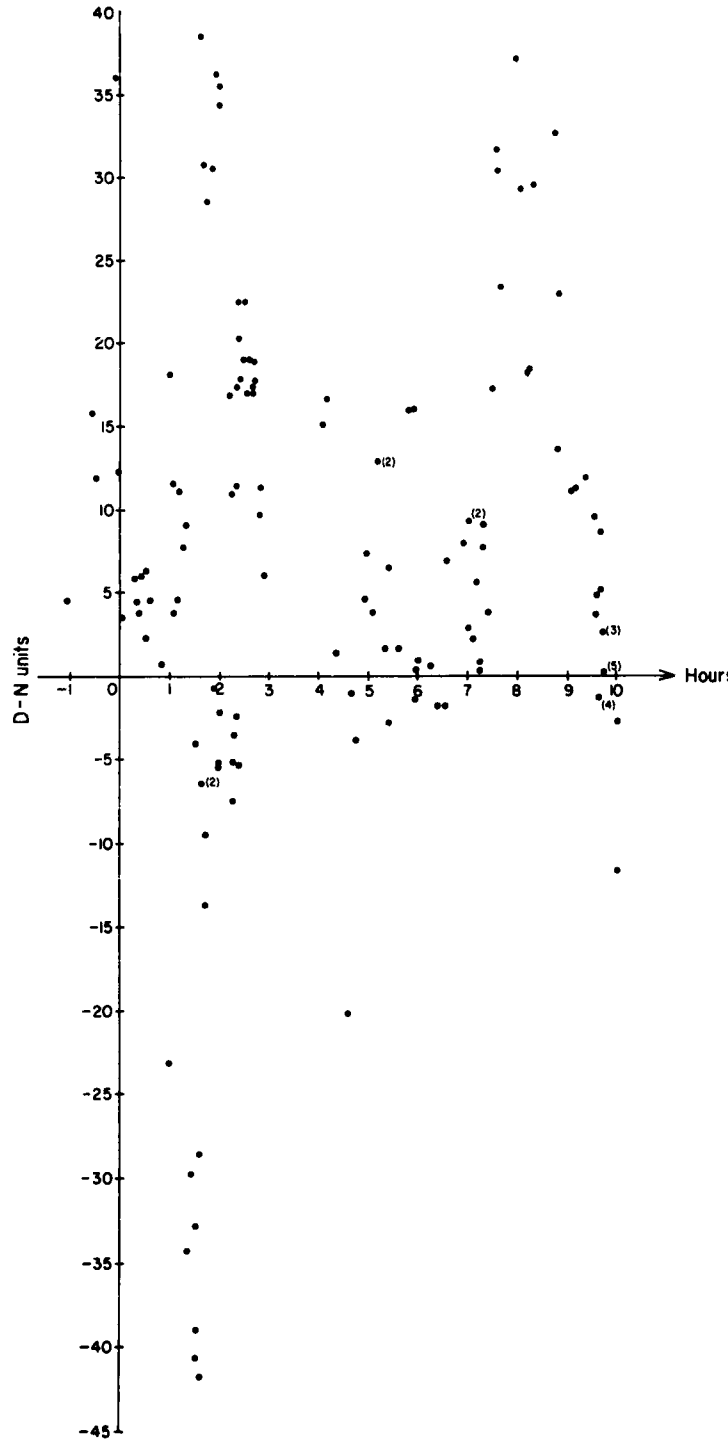

Fig. 37. D versus lapse of time from radiosonde observation to cloud measurement.

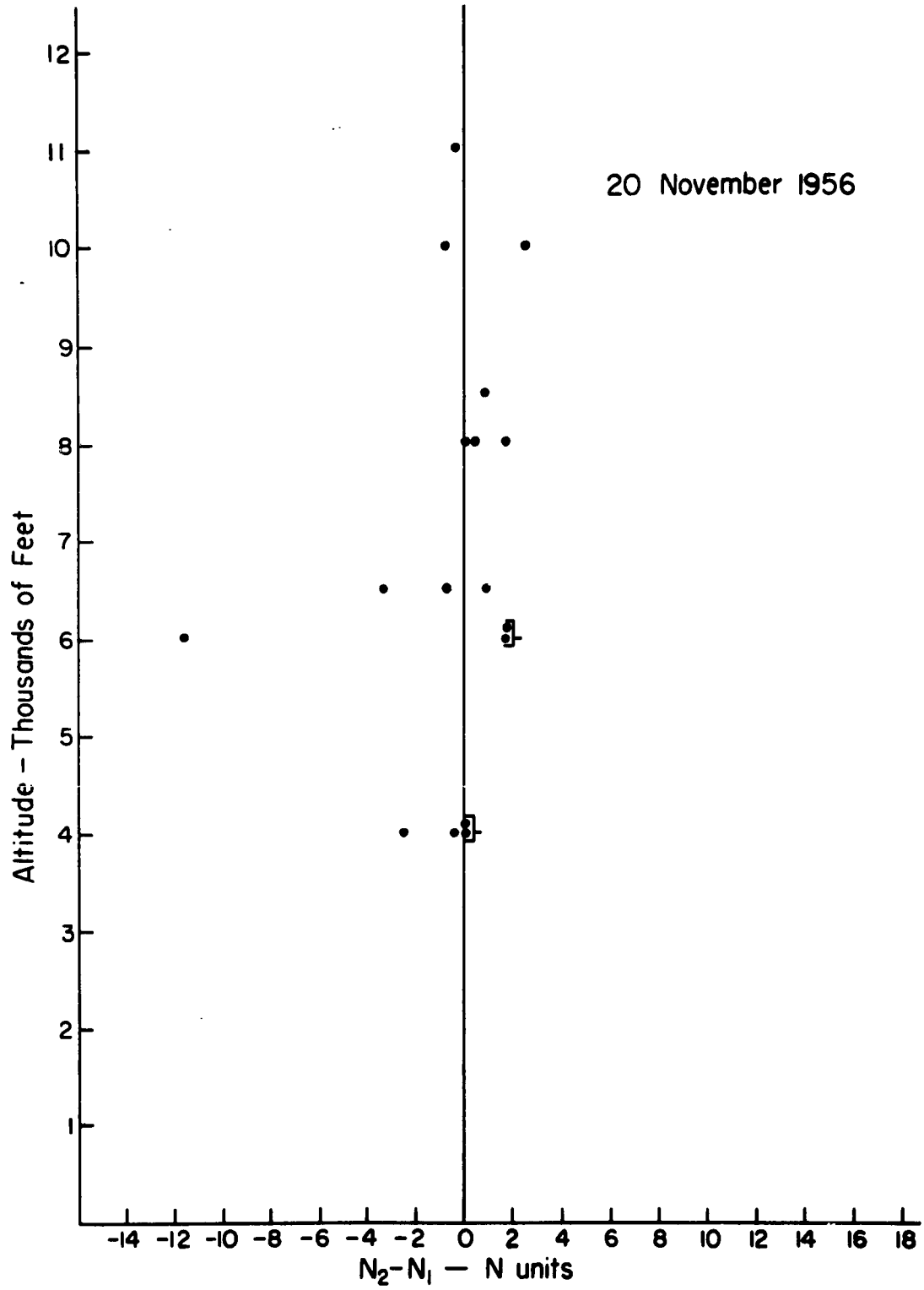
20 November 1956
Altitude - Thousands of Feet
12
11
10
9
8
7
6
5
4
3
2
1
-14 -12 -10 -8 -6 -4 -2 0 2 4 6 8 10 12 14 16 18
N2-N1 — N units

Fig. 38.

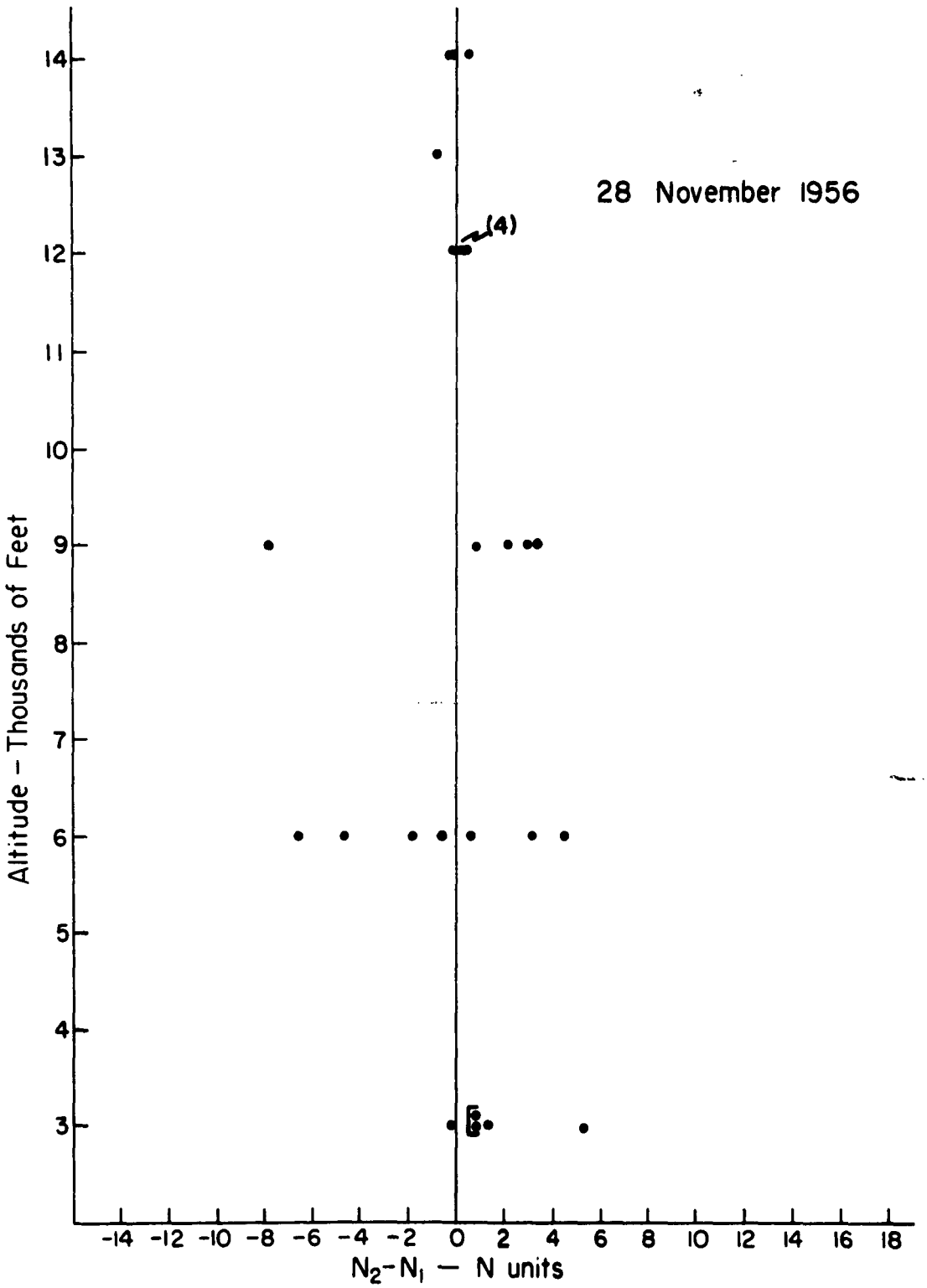
28 November 1956
(4)
Altitude – Thousands of Feet
14
13
12
11
10
9
8
7
6
5
4
3
-14 -12 -10 -8 -6 -4 -2 0 2 4 6 8 10 12 14 16 18
N2-N1 — N units

Fig. 39.

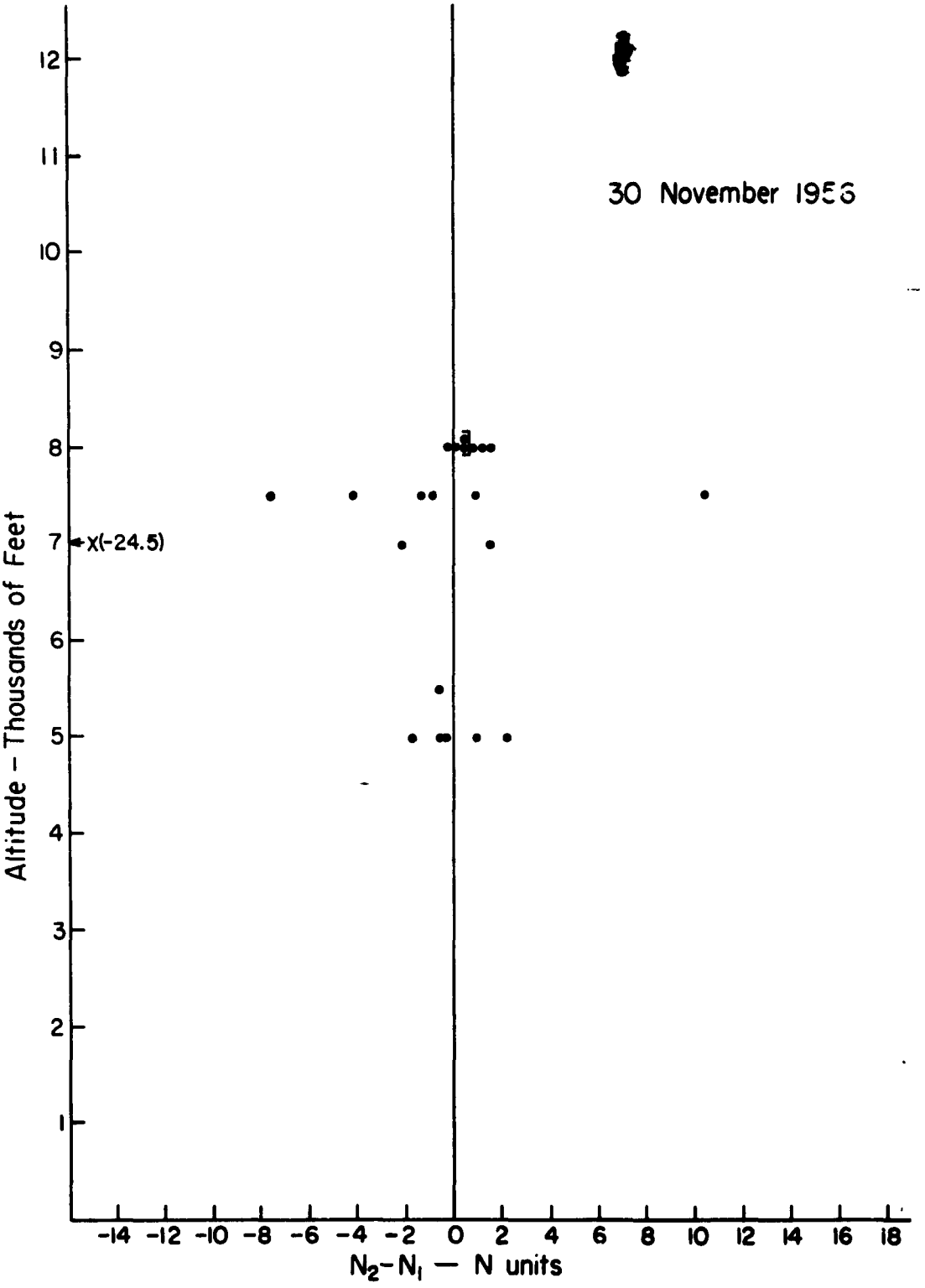
30 November 1953
Altitude - Thousands of Feet
12
11
10
9
8
7
6
5
4
3
2
1
X(-24.5)
-14 -12 -10 -8 -6 -4 -2 0 2 4 6 8 10 12 14 16 18
N2-N1 — N units

Fig. 40.

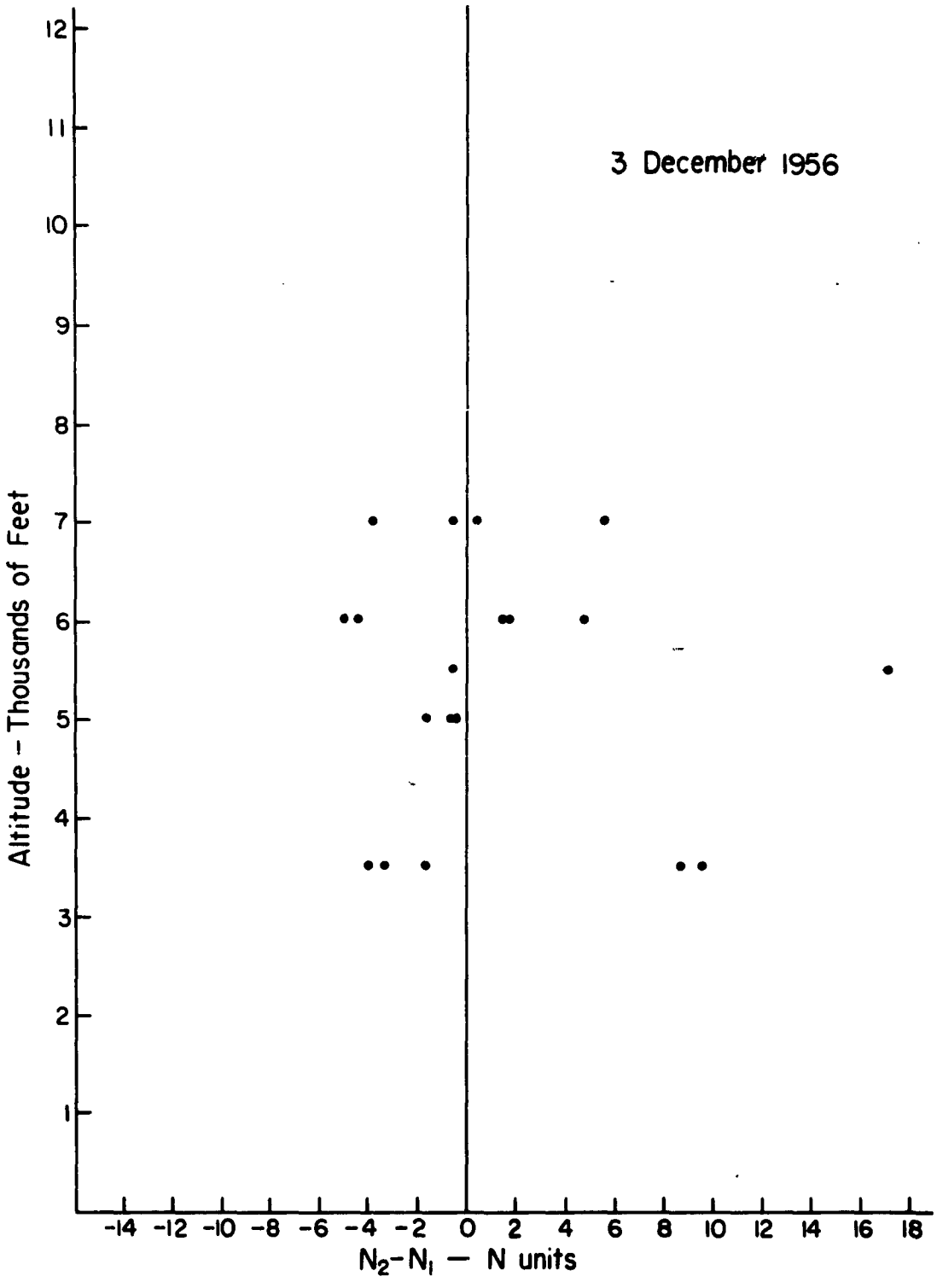
3 December 1956
Altitude - Thousands of Feet
12
11
10
9
8
7
6
5
4
3
2
1
-14 -12 -10 -8 -6 -4 -2 0 2 4 6 8 10 12 14 16 18
N2-N1 — N units

Fig. 41.

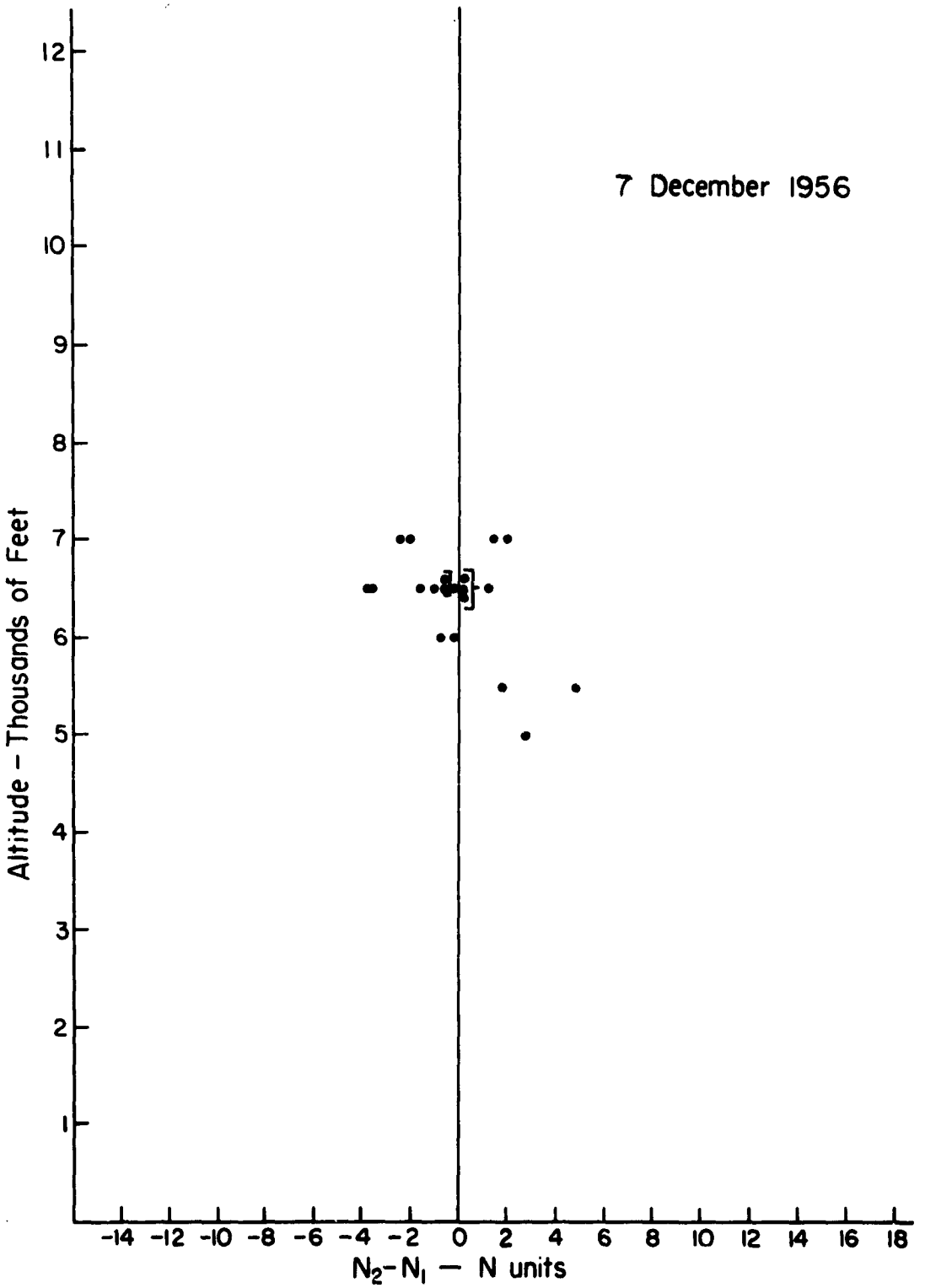
7 December 1956
Altitude – Thousands of Feet
12
11
10
9
8
7
6
5
4
3
2
1
-14 -12 -10 -8 -6 -4 -2 0 2 4 6 8 10 12 14 16 18
N2-N1 — N units

Fig. 42.

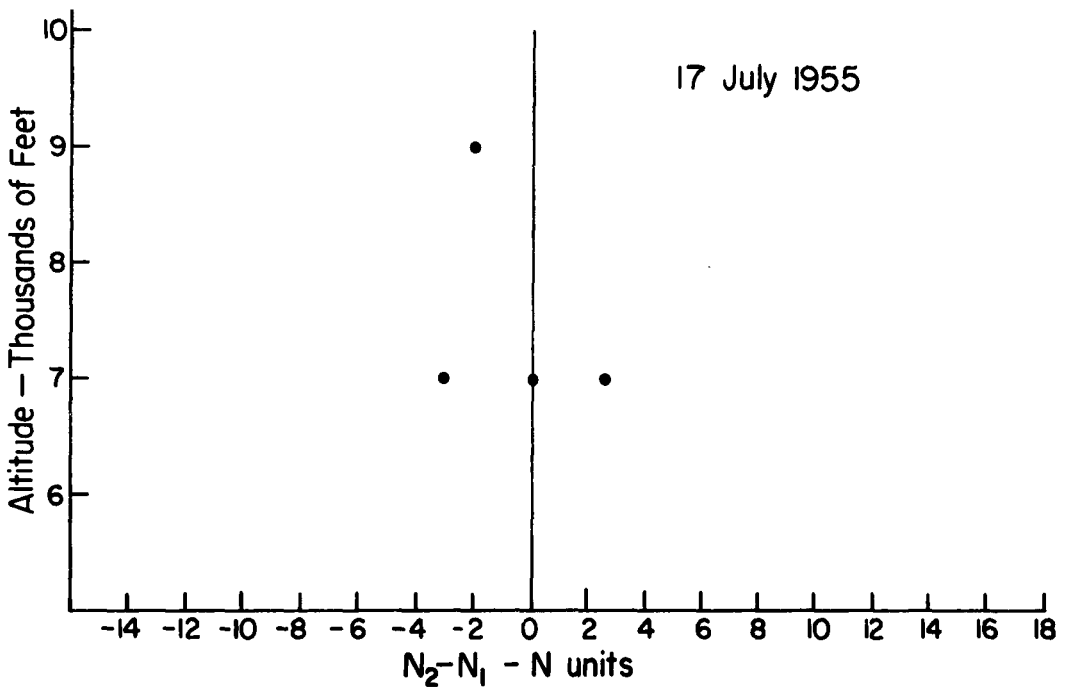
17 July 1955
Altitude – Thousands of Feet
10
9
8
7
6
-14 -12 -10 -8 -6 -4 -2 0 2 4 6 8 10 12 14 16 18
N_2-N_1 - N units

Fig. 43.

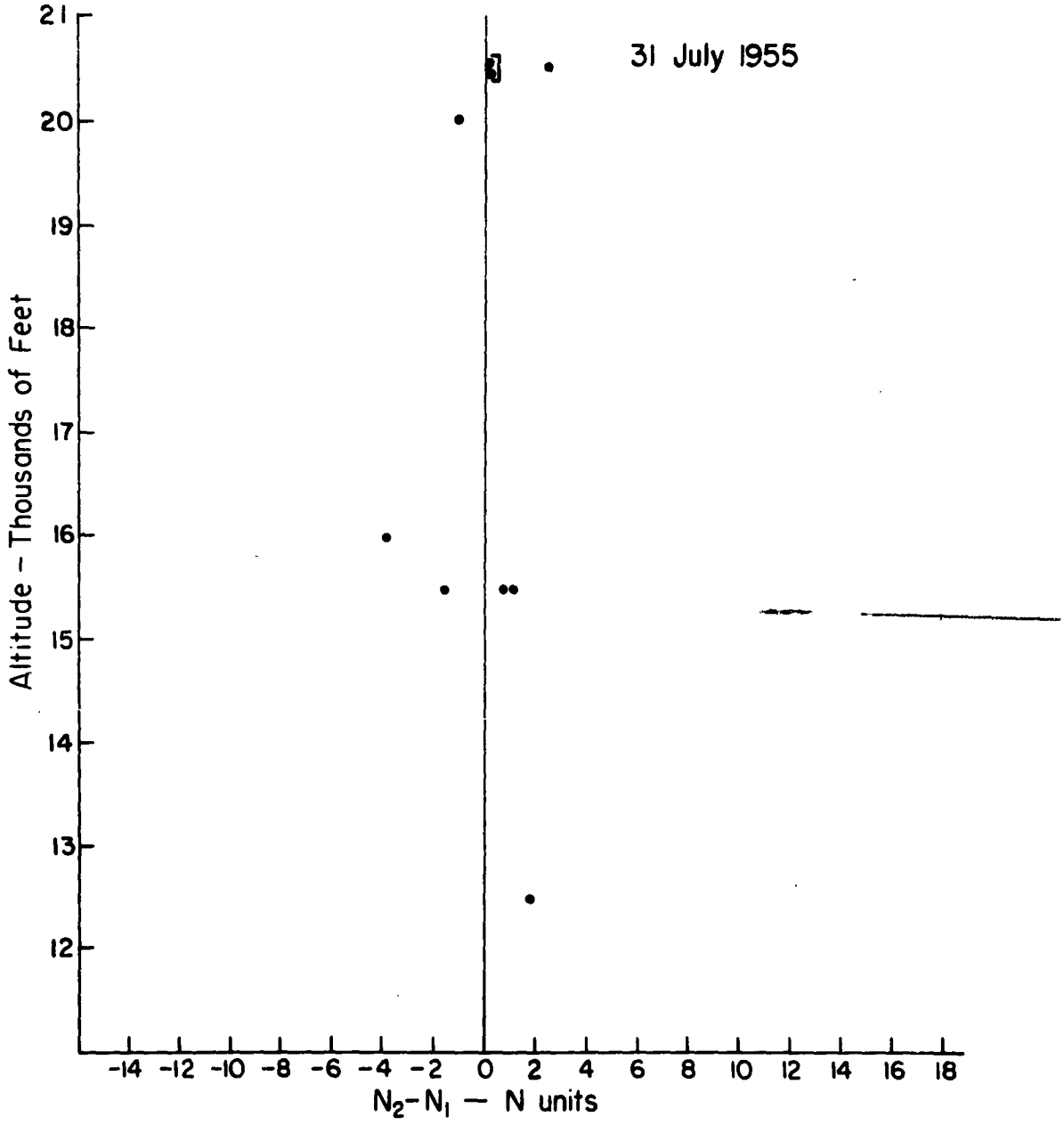
31 July 1955
Altitude - Thousands of Feet
21
20
19
18
17
16
15
14
13
12
-14 -12 -10 -8 -6 -4 -2 0 2 4 6 8 10 12 14 16 18
N2 - N1 — N units

Fig. 44.

APPENDIX A

The refractive index gradient data from the seven low altitude passes are presented in the following two tables, one for clear air measurements and one for cloud measurements. The tables are bivariate frequency distributions of ΔN, the abscissa, versus ΔS, the ordinate. The class intervals of ΔN are in N units, those of ΔS in meters.

Clear Air

Δs	ΔN 0.0 -0.4	0.5 -0.9	1.0 -1.4	1.5 -1.9	2.0 -2.4	2.5 -2.9	3.0 -3.4	3.5 -3.9	Total
0.0 -2.49	915	427	39	6	1				1388
2.5 -4.99	1266	510	52	17	6	2		1	1854
5.0 -7.49	935	302	42	11	1	3	1		1295
7.5 -9.99	619	188	20	4		1			832
10.0 -12.49	383	88	10	2	2				485
12.5 -14.99	192	62	11	1	1				267
15.0 -17.49	163	32	7	1	1			1	205
17.5 -19.99	138	20	2	2					162
20.0 -22.49	143	21	2						166
22.5 -24.99	44	10	2	1					57
25.0 -27.49	38	5	1						44
27.5 -29.99	28	6							34
30.0 -32.49	24	2	1						27
32.5 -34.99	22								22
35.0 -37.49	5	3	1						9
37.5 -39.99	14		1						15
40.0 -42.49	11		1						12
42.5 -44.99	27	2							29
45.0 -47.49	12	3							15
47.5 -49.99	11	1							12
Total	4990	1682	192	45	12	6	1	2	6930

Cloud Air

Δ s	Δ N 0.0 -0.4	0.5 -0.9	1.0 -1.4	1.5 -1.9	2.0 -2.4	2.5 -2.9	3.0 -3.4	3.5 -3.9	Total
0.0 -2.49	1196	572	113	31	9	4	1		1926
2.5 -4.99	2035	881	149	39	6	6	2	2	3120
5.0 -7.49	1250	467	65	11	4			1	1798
7.5 -9.99	879	175	24	3	2	1		1	1085
10.0 -12.49	368	93	11	3					475
12.5 -14.99	185	29	5		1				220
15.0 -17.49	80	17	2						99
17.5 -19.99	58	12	3						73
20.0 -22.49	38	4		1					43
22.5 -24.99	24	4							28
25.0 -27.49	7								7
27.5 -29.99	9		1						10
30.0 -32.49	8								8
32.5 -34.99	2								2
35.0 -37.49	1								1
37.5 -39.99	2	1							3
40.0 -42.49	2								2
42.5 -44.99		1							1
45.0 -47.49	2								2
47.5 -49.99	3								3
Total	6149	2256	373	88	22	11	3	4	8906

APPENDIX B

Fig. 45 through 49 present certain refractive index features of some illustrated clouds. The clouds were selected from the late 1956 flights over the Caribbean. The photographs were made between 15 and 30 sec prior to cloud entry by the aircraft.

Graphs in each figure show respectively the refractometer record through the cloud and $\int \Delta N dS$ for the first 300 m of cloud flight path. In the graph of the refractive index record zero on the ordinate scale represents environment refractive index (N_1 in fig. 28) and zero on the abscissa scale is the edge of the cloud.

Of the five cloud faces which are illustrated, only the one in fig. 46 has what would be termed a hard appearance. This hardness is reflected in a small transition zone and an integral function which increases rather rapidly.

Soft, fleecy cloud faces and associated active transition zones are demonstrated in fig. 45 and 47. The cloud in fig. 49 is growing into very dry environment air, as evidenced by the large value of $N_c - N_1$. The integral function for this cloud is consequently very large.

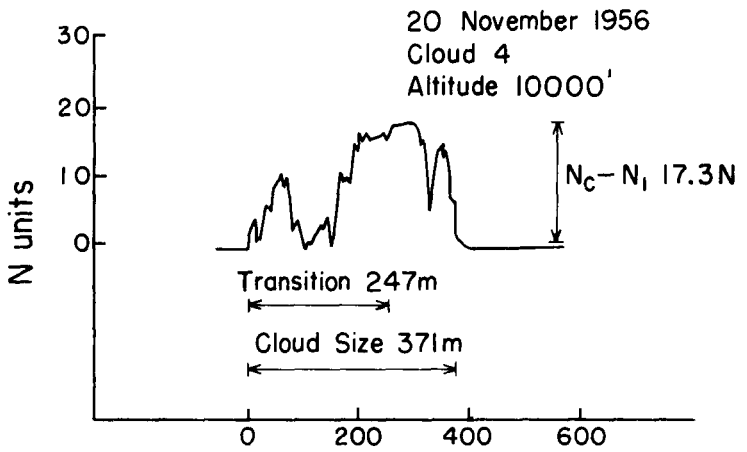
20 November 1956
Cloud 4
Altitude 10000'
30
20
10
0
N units
$N_C - N_I$ 17.3N
Transition 247m
Cloud Size 371m
0
200
400
600

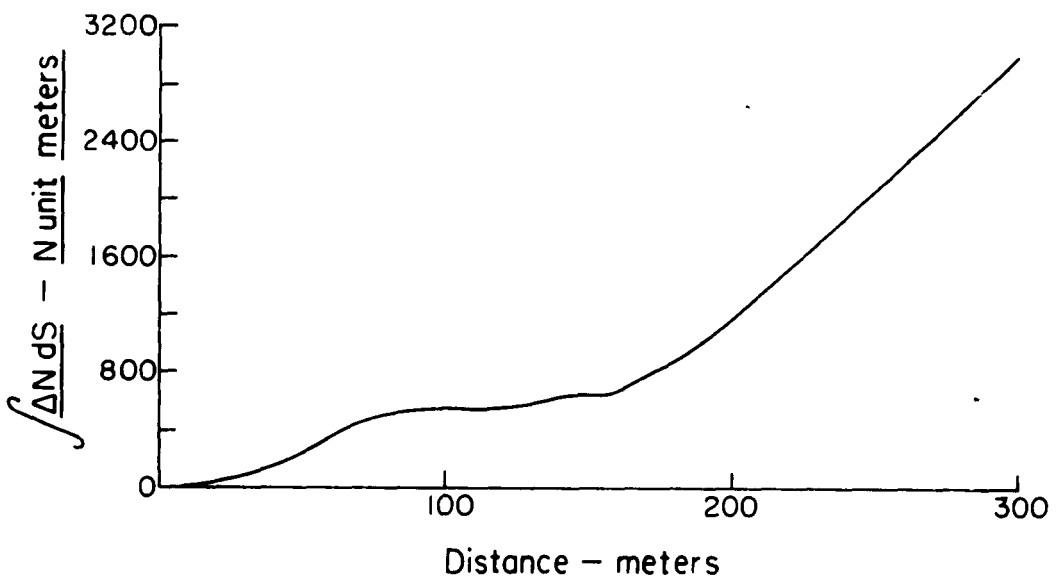
3200
2400
1600
800
0
$\int \Delta N\, dS$ – N unit meters
100
200
300
Distance – meters

Fig. 45

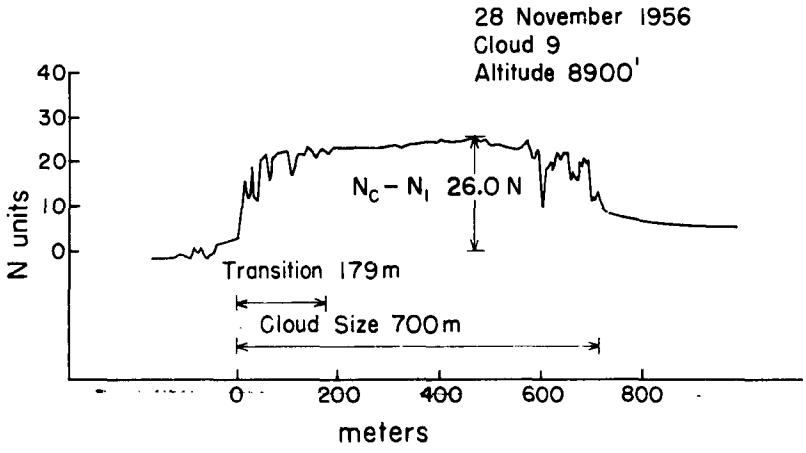
28 November 1956
Cloud 9
Altitude 8900'
N units
40
30
20
10
0
$N_c - N_1$ 26.0 N
Transition 179m
Cloud Size 700m
0
200
400
600
800
meters

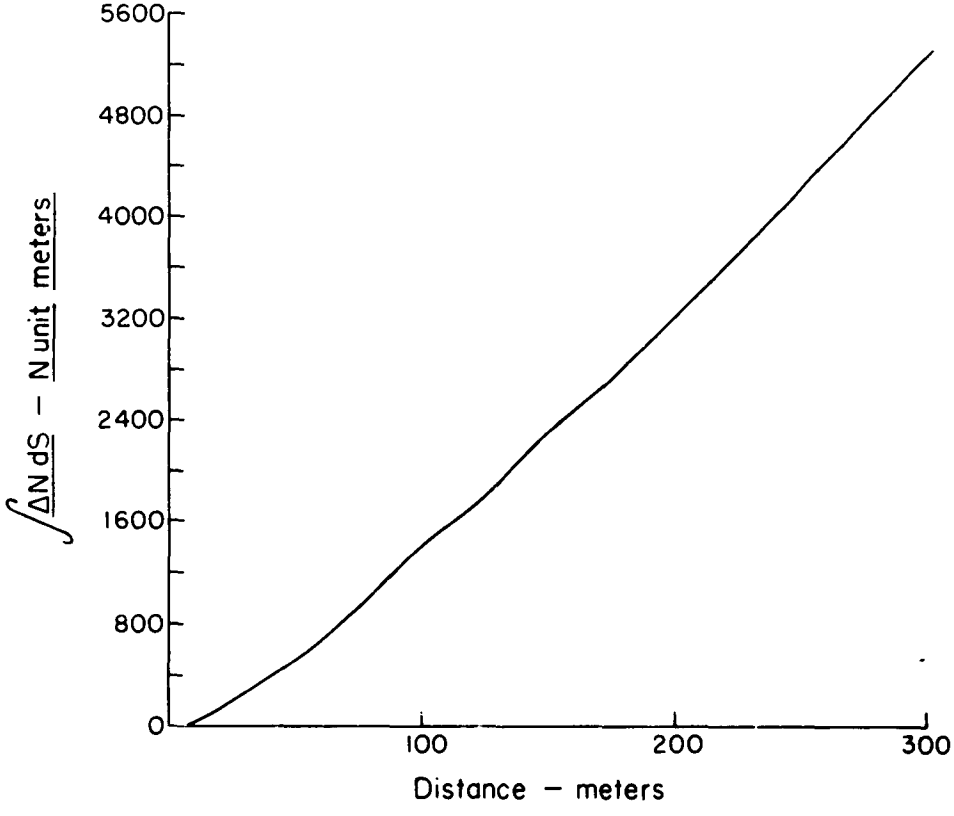
$\int \Delta N\, dS$ – N unit meters
5600
4800
4000
3200
2400
1600
800
0
100
200
300
Distance – meters

Fig. 46

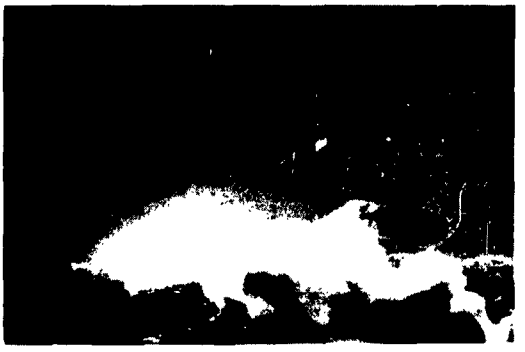

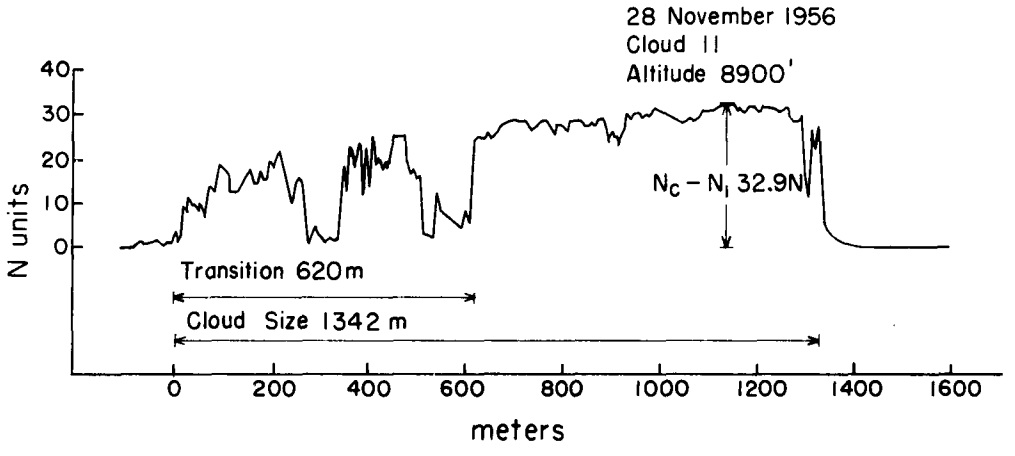
28 November 1956
Cloud 11
Altitude 8900'
N units
40
30
20
10
0
$N_c - N_i$ 32.9N
Transition 620m
Cloud Size 1342 m
0
200
400
600
800
1000
1200
1400
1600
meters

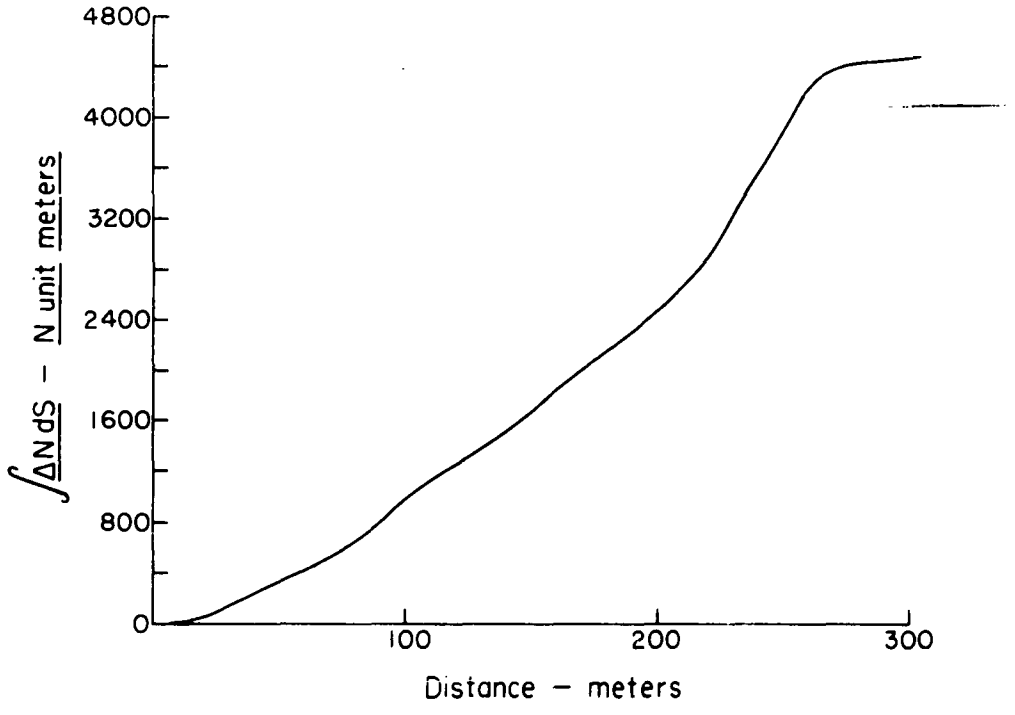
$\int \Delta N\, dS$ - N unit meters
4800
4000
3200
2400
1600
800
0
100
200
300
Distance - meters

Fig. 47

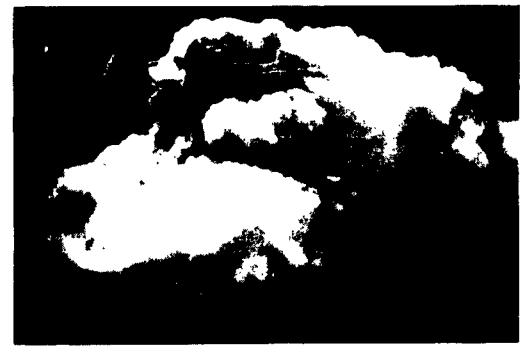

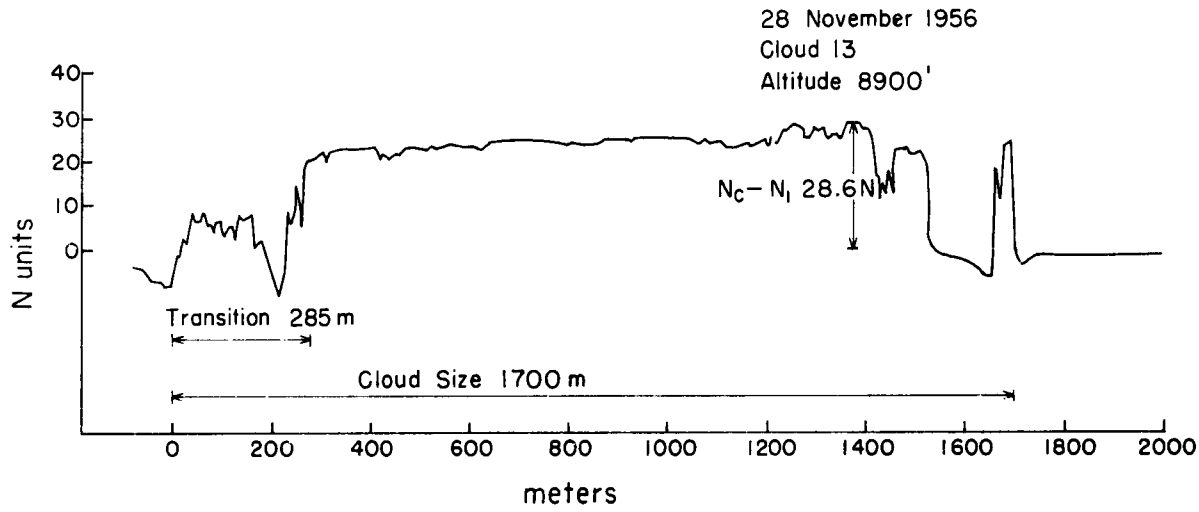
28 November 1956
Cloud 13
Altitude 8900'
N units
40
30
20
10
0
$N_C - N_I$ 28.6N
Transition 285 m
Cloud Size 1700 m
0
200
400
600
800
1000
1200
1400
1600
1800
2000
meters

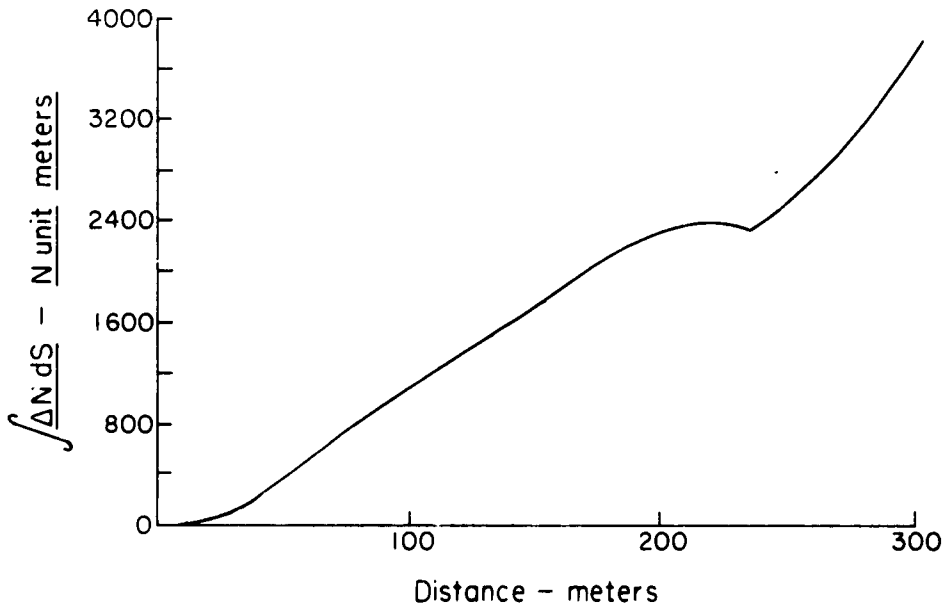
$\int \Delta N\, dS$ - N unit meters
4000
3200
2400
1600
800
0
100
200
300
Distance - meters

Fig. 48

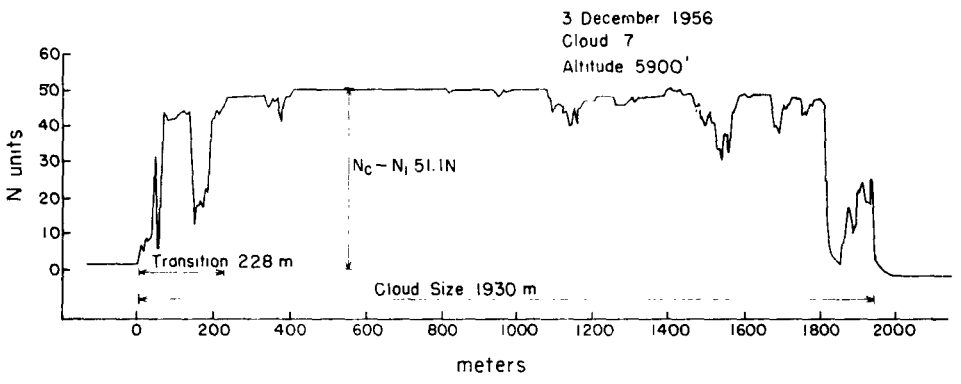
3 December 1956
Cloud 7
Altitude 5900'
N units
60
50
40
30
20
10
0
$N_c - N_i$ 51.1N
Transition 228 m
Cloud Size 1930 m
0
200
400
600
800
1000
1200
1400
1600
1800
2000
meters

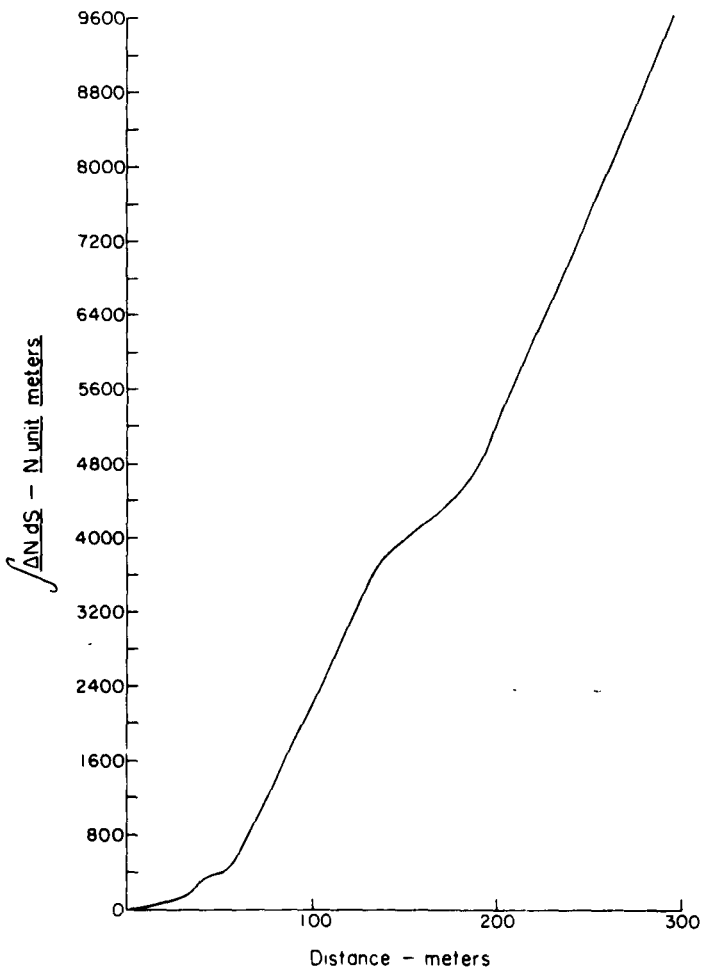
$\int \Delta N\, dS$ – N unit meters
9600
8800
8000
7200
6400
5600
4800
4000
3200
2400
1600
800
0
100
200
300
Distance – meters

Fig. 49

APPENDIX C

ON FINDING THE EDGE OF A CLOUD

In evaluating cloud measurements made by airborne instruments, the analyst first must identify his cloud data. He may do this qualitatively by observing the behavior of the record of his instruments, knowing from experience their characteristic behavior in and out of cloud. Quantitative information about the location of the measuring aircraft with respect to the cloud can be supplied by an observer on the aircraft. A common practice is to have the observer apply an electrical signal to the data records as the aircraft enters a cloud and another signal as the aircraft passes from cloud air to environment air. This technique was employed on the data gathering flights treated in this report.

The accuracy of determination of the time of aircraft entry into a cloud from the observer's signal is subject to several human frailties, the commonest of which are error of judgment and delay in putting the signal on the record. The behavior of the refractometer as the aircraft passes through a cloud boundary is such that in a large number of cases it indicates the cloud edge quite precisely. Indeed, the cloud as defined by the record trace of the refractometer has formed the foundation for the analysis presented in this report. In a large number of cases the temperature record provided by a platinum resistance thermometer in a vortex housing also has shown a characteristic deflection at the cloud

edge. We present here a comparison of the abilities of the observer and the instruments to detect the boundary of a cloud.

Data from seven of the over-water flights were examined and 73 clouds were chosen in which there was no doubt about the inbound cloud boundary as shown by the refractometer. For each cloud three values of time were recorded: t_o the time of cloud entry as indicated by the observer's signal; t_r the time of the step in the refractive index record associated with cloud entry, and t_v the time of the vortex temperature deflection due to cloud penetration. The three time differences associated with these measurements were then computed. Fig. 50 shows the frequency distribution of $t_r - t_o$, the time difference between cloud edge as indicated by the refractometer and cloud edge as indicated by the observer. Table 15 presents the means and variances of the distribution of the three time difference measurements.

TABLE 15. MEANS AND VARIANCES OF THE DISTRIBUTION OF THE TIME DIFFERENCES AMONG t_r, t_o, and t_v

Statistic	Mean	Variance
$t_r - t_o$	-0.08 sec	0.808
$t_r - t_v$	-0.02 sec	0.005
$t_o - t_v$	-0.06 sec	0.808

It is evident from the table that the observer's cloud signal provides most of the variance in the distributions in which it is involved.

Fig. 50 thus presents a picture of the ability of a passenger on an aircraft to make a record of the time when the aircraft enters a cloud under favorable conditions at B-29 air speeds. Favorable conditions are best exemplified by fig. 46, where, at the point of aircraft entry, the cloud face appears hard and satellite cloud or scud is absent. Under such conditions the difficulty in deciding when the aircraft passes through the cloud boundary should be at a minimum and most of the variance of the distribution in fig. 50 should be attributable to the observer's reaction time. The t-test affirms that the sample of $t_r - t_o$ came from a population with a mean of zero, indicating that the airborne observer anticipates the cloud edge to the same degree that he lags it. The data represent more than one observer and no attempt has been made to examine individual behavior characteristics.

The standard deviation of the distribution of $t_r - t_o$ is 0.9 sec. At B-29 air speeds this represents $\pm$ 90 m of flight path. How much this might increase for clouds with diffuse edges we can only guess. The study seems to speak rather strongly in favor of using the refractometer as a cloud indicating device.

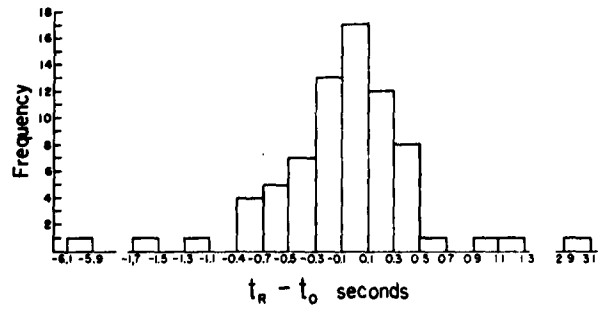
Frequency
2
4
6
8
10
12
14
16
18
-6.1 -5.9
-1.7 -1.5 -1.3 -1.1 -0.4 -0.7 -0.5 -0.3 -0.1 0.1 0.3 0.5 0.7 0.9 1.1 1.3
2.9 3.1
$t_R - t_o$ seconds

Fig. 50.